Review

Reconfigurable Metasurface: A Systematic Categorization and Recent Advances

Changhao Liu[1,2], Fan Yang[1,2], Shenheng Xu[1,2], and Maokun Li[1,2]

1. *Department of Electronic Engineering, Tsinghua University, Beijing 100084, China*
2. *Beijing National Research Center for Information Science and Technology* (*BNRist*), *Beijing 100084, China*

Corresponding author: Fan Yang, Email: fan_yang@tsinghua.edu.cn.

Abstract — Considering the rapid progress of theory, design, fabrication and applications, metasurfaces (MTSs) have become a new research frontier in microwave, terahertz and optical bands. Reconfigurable metasurfaces (R-MTSs) can dynamically modulate electromagnetic (EM) waves with unparalleled flexibility, which has led to a great surge of research in recent years. Numerous R-MTSs with powerful capabilities and various functions are being proposed explosively. Based on the five dimensions of EM waves, this review proposes a unified model to describe the interactions among R-MTSs, EM waves and EM information and suggests an information bit allocation strategy to categorize different types of R-MTSs systematically. Recent advances in R-MTSs and 1-bit and 2-bit elements manipulating different wave dimensions are reviewed in detail. Finally, this review discusses the future research trends of R-MTSs. R-MTSs with diverse dimensions and functions may propel the next generation of communication, detection, sensing, imaging and computing applications.

I. Introduction

Electromagnetic (EM) waves are the cornerstone of modern society. For purpose of manipulating EM waves, metasurfaces (MTSs), as artificial arrays composed of ultrathin subwavelength elements, have been invented and studied over the decades. MTSs can manipulate multidimensional EM waves with an unparalleled degree of freedom. Moreover, compared with conventional bulk devices used for manipulating EM waves, MTSs have great advantages such as low cost, low profile, light weight, high efficiency and easy fabrication. Therefore, MTSs are currently attracting tremendous interest from researchers, and the applications around MTSs are experiencing explosive growth, such as high-performance antennas [1], radar cross sections (RCSs) reducing radomes [2], invisibility cloaks [3], holograms [4], [5], and ultrathin lenses [6].

Evolving from conventional MTSs, reconfigurable metasurfaces (R-MTSs) integrated with tunable materials on each element show a dynamic capability to control EM waves. The scattering patterns of EM waves after encountering an R-MTS can be tuned by applying input stimuli to the R-MTS. Various types of R-MTSs have been proposed with reconfigurable functions for tuning different dimen-sions of EM waves. Moreover, state-of-the-art prototypes are emerging with multiplexed functions on a single R-MTS, indicating that the research on R-MTSs is evolving toward multiple dimensions and multiple functions. Some review articles on passive and active metasurfaces can be found in [7]–[12].

Digital R-MTSs, which are reconfigurable forms of the coding metasurfaces [13], have sparked significant research interest. By incorporating lumped switches with discrete control signals on MTSs, significant advantages are obtained over conventional analog R-MTSs, such as low cost, ease of manipulation, scalability, high reliability, and compatibility with the information world. As a result, this review primarily focuses on digital R-MTSs, which are characterized by information bits.

A digital R-MTS not only shapes the physical EM wave and guides the flow of EM energy but also modulates the incident wave and generates information. Information is encoded onto the EM wave and can take various forms depending on the dimensions of the EM wave. As a result, R-MTSs have additional functions and capabilities for manipulating multiple dimensions of EM waves, leading to a significant surge in R-MTS research.

With tremendous advantages and revolutionary applications, numerous R-MTSs with diverse functions are being developed. However, corresponding to these functions, various terminologies have emerged, making the structure of R-MTS research appear complex and confusing. Hence, there is a need for systematic categorization of R-MTSs. In this regard, we propose a unified mathematical model of R-MTSs based on five dimensions of EM waves to describe the interactions among R-MTSs, EM waves, and EM information. We then introduce the information allocation strategy, which aims to reorganize these R-MTSs under a unified terminology system. By employing this systematic categorization, we review recent advances in R-MTSs within the same terminology system. This strategy could significantly contribute to the development of surface electromagnetics theory [14]. We hope that this review provides a comprehensive understanding of R-MTSs, EM waves, EM information as well as their interactions while inspiring researchers to further explore the fascinating functions of R-MTSs.

This remainder of this review is organized as follows. First, we focus on the interactions among EM waves, EM information and R-MTSs, and propose an information allocation strategy in Section II. Next, under the framework of information allocation, we review different forms of 1-bit allocation elements in Section III. Continuing from that perspective, Section IV primarily reviews 2-bit allocation elements. Then in Section V, we discuss the future trends of R-MTSs and outline some challenges. Finally, we draw our conclusions in Section VI.

II. Information Allocation Strategy

1. Dimensions of the EM wave

First, it is necessary to review the dimensions of the plane EM wave. A plane EM wave can be mathematically described using the following formula:

$$\vec{E}(t,\vec{r}) = E_0 e^{j(\omega t - \vec{k}\cdot\vec{r}+\varphi)}|p\rangle \qquad (1)$$

This formula involves five dimensions of plane EM waves: phase (φ), amplitude (E_0), polarization ($|p\rangle$), direction ($\vec{k}$) and frequency (ω). Note that since the field is polarized, $\vec{E}$ is a vector and is also a function of space ($\vec{r}$) and time (t).

2. Interactions among the R-MTS, wave and information

To understand the functions of the R-MTS, the physical point of view is initially considered. When the EM wave encounters an R-MTS, each element of the R-MTS scatters the local EM wave. Then, the scattered EM waves propagate in free space. Summing up the contributions of each local scattered EM wave, the receiver obtains the final EM response. The R-MTS possesses dynamic control over EM waves in five dimensions, enabling the manipulation of wave–metasurface interactions.

Considering the information viewpoint, we can gain an alternative understanding of the functions of the R-MTS. Our focus in this review is primarily on digital information, which plays a fundamental role in the modern world and is characterized by its binary nature. In comparison to analog information, digital information offers robustness, speed, cost-effectiveness, and ease of processing, making it increasingly important.

To generate and transmit digital EM information in free space, the physical information medium, the EM wave, is indispensable. Since EM waves have five dimensions, EM information has five dimensions. The R-MTS is designed for the purpose of manipulating EM waves, which in turn allows for the modulation of EM information with diverse dimensions. Thus this type of R-MTS is multidimensional. Figure 1 illustrates the interactions among the R-MTS, EM wave and EM information, linked by EM dimensions.

Based on the information point of view, the R-MTS provides dynamic control of the information–metasurface interactions. The R-MTS can not only manipulate physical EM waves but also generate and modulate EM information. Because it bridges the physical and information realms, the R-MTS is called an information metasurface [15].

3. Mathematical model of the R-MTS

Here, we propose a mathematical model of the R-MTS to describe the interactions among the R-MTS, EM wave and EM information. Suppose an R-MTS is composed of M elements. When an EM wave encounters the R-MTS, the scattered wave is represented by the following formula:

$$\vec{E}^{\text{sca}}(t,\vec{r}) = \sum_{i=1}^{M} \mathbb{P}_i(\vec{r}) \cdot \mathbb{M}_i(t,\vec{r},R_i) \cdot \vec{E}_i^{\text{inc}}(t,\vec{r}_i) \qquad (2)$$

where inc represents the incident wave and sca represents the scattered wave. The location of the receiver is denoted by $\vec{r}$, and $\vec{r}_i$ represents the position of the ith element. Here, $\vec{E}_i^{\text{inc}}$ is the incident wave at the ith element. Note that the incident wave is not necessarily a plane wave, but it is assumed that at a small local region of each element, the incident wave can be approximated as a plane wave. According to formular (1), $\vec{E}_i^{\text{inc}}$ can be expressed as

$$\vec{E}_i^{\text{inc}}(t,\vec{r}_i) = E_{0i}^{\text{inc}} e^{j(\omega_i^{\text{inc}} t - \vec{k}_i^{\text{inc}}\cdot\vec{r}_i + \varphi_i^{\text{inc}})}|p_i^{\text{inc}}\rangle \qquad (3)$$

with variable values of the incident dimensions at each element in different positions.

$\mathbb{M}_i(t,\vec{r},R_i)$ represents the ith element modulation matrix of the incident wave, and the notation

$$R_i = (\vec{E}_i^{\text{inc}}, \text{Switch}_i) \qquad (4)$$

is used to describe the response of the elements. R_i contains the incident dimensions of the EM wave and the element configurations determined by the switch. We call the former *excitation* and the latter *control*. It is also noted that R_i is a function of time t because Switch$_i$ can be modulated
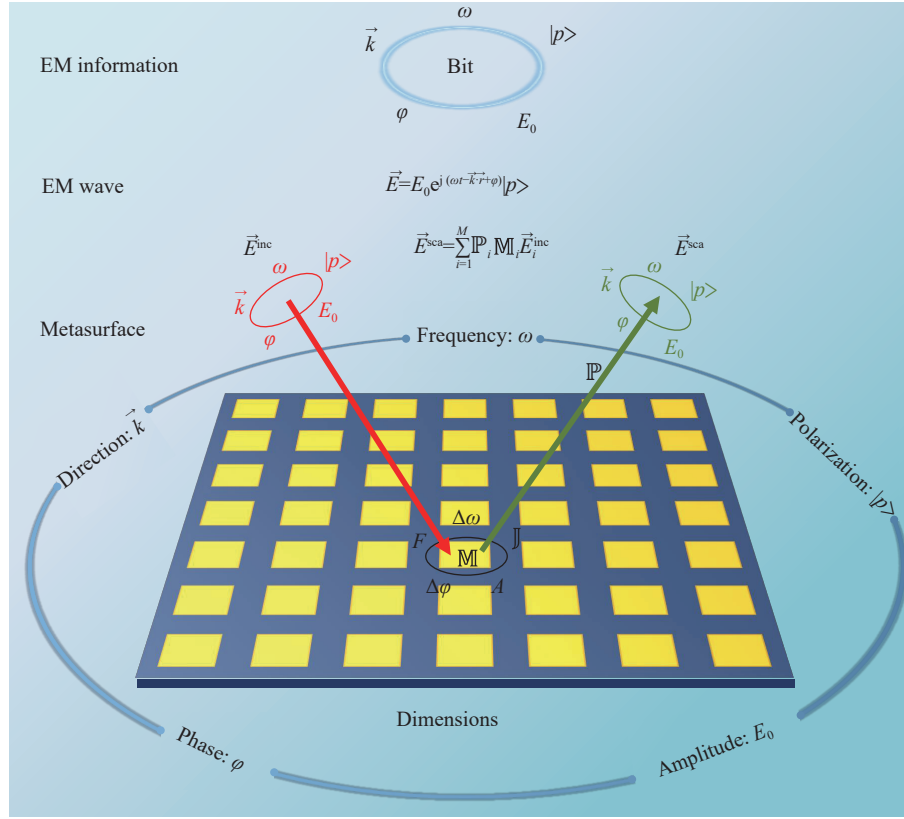
Figure 1 An illustration of the information allocation strategy and the interactions among EM information, EM waves and R-MTSs, which are linked by EM dimensions. Since EM waves have five dimensions, EM information bits can be allocated to these dimensions. When a five-dimensional incident EM wave encounters an R-MTS, it is modulated by a modulation matrix $\mathbb{M}$ for each element. This modulation matrix manipulates the five EM dimensions and loads EM information onto the EM wave. After propagating through free space, the total scattered wave in the far field is the sum of all scattered waves from each element. In summary, the information to be transmitted is allocated to the dimensions of the scattered EM wave and dynamically modulated by the R-MTS.

temporally, which is the underlying mechanism of reconfiguration.

$\mathbb{M}_i(t, \vec{r}, R_i)$ is expressed as

$$\mathbb{M}_i(t, \vec{r}, R_i) = A_i(R_i) F_i(\vec{r}, R_i) e^{j(\Delta\omega_i(R_i)t + \Delta\varphi_i(R_i))} \mathbb{J}_i(R_i) \qquad (5)$$

In this equation, the amplitude response (A) describes the states of energy amplification, attenuation, or maintenance. The element radiation pattern (F) depends on the receiving location ($\vec{r}$) and can shape the beam and determine its direction. The additional frequency ($\Delta\omega$) can shift the incident frequency, which is a nonlinear effect. The additional phase shift ($\Delta\varphi$) accounts for the phase shifting effect when the incident wave encounters the EM element. The Jones polarization matrix ($\mathbb{J}$) is an 2×2 anisotropic matrix that modulates the incident polarization ($|p^{\mathrm{inc}}\rangle$), and accordingly, $\mathbb{M}$ is also an 2×2 matrix. These five dimensions of element modulation precisely cover and modulate the five dimensions of the EM wave.

The term $\mathbb{P}_i(\vec{r})$ describes the path from the R-MTS to the information receiver. Suppose the path is linear, time-invariant, isotropic, homogeneous and singular; then, the mathematical model can be expressed as

$$\mathbb{P}_i(\vec{r}) = L_i(\vec{r}) e^{-j\vec{k}\cdot(\vec{r}-\vec{r}_i)} \mathbb{I} \qquad (6)$$

where L_i denotes the path loss from the ith element to the receiver and $\mathbb{I}$ is the polarization identity matrix. The path model is determined by the location of the information receiver ($\vec{r}$) and the position of each element ($\vec{r}_i$).

Each element can exhibit different responses to different dimensions of the incident wave. Furthermore, as the elements can be reconfigured in multiple dimensions, these dimensions of the EM wave can be dynamically modulated. By summing the individual element responses, the EM wave scattered by the R-MTS is obtained according to (2).

4. Information allocation strategy: Element level

As shown in (2), the characteristics of the R-MTS are determined by EM elements. Suppose N-bit information (2^N states) needs to be generated by an EM element. Since EM information resides in the EM wave, the N-bit information can be allocated to different dimensions of the EM wave. Correspondingly, these dimensions of the EM wave need to be independently modulated by the element, and each element has to respond to the desired dimensions of the EM wave. The key to transmitting multidimensional EM information is designing multidimensional reconfigurable elements. This is why this strategy is named *information bit allocation*, signifying the allocation of multidimensional EM

information bits to multidimensional reconfigurable EM elements. By employing this strategy, researchers can determine the categories of various reconfigurable elements and gain a better understanding of the functionalities associated with each type of reconfigurable element.

5. Information allocation strategy: Array level

In addition to element-level reconfiguration, there is also an array-level information allocation strategy to be considered. Strictly speaking, the overall electromagnetic response is the sum of each element's contribution to the different dimensions. Since there are M independent elements in an R-MTS and each element manipulates N independent bits, the total number of modulated bits within the entire R-MTS is given by $M \times N = K$, hence it can greatly multiply the amount of information.

Considering the effect of the array, the arrangement and state of each element at the array level also require careful design, which is referred to as array-level bit allocation. By manipulating the states of each element within the array, a diverse range of waveform patterns can be generated, such as pencil beams, monopulse patterns, multiple beams, orbit angular momentum (OAM) beams, and RCS reduction [16]–[19]. Additionally, the polarization states, beam amplitude, beam direction, and frequency components can be quasicontinuously controlled by adjusting the states of the multidimensional elements at the array level. The realization of such functions requires specific strategies to allocate the K bits to different dimensions, thus leading to research on of array-level bit allocation strategies.

In this review, our primary focus is on element-level reconfigurable element design due to its importance and fundamentality. The array-level bit allocation strategy is more complex and flexible, and it is beyond the scope of this review.

6. Element control methods

The composition of the R-MTS relies on EM elements, and their reconfiguration is facilitated by the use of tunable devices/materials. These EM elements can be controlled using different stimuli, including electrical control [20], mechanical control [21], [22], temperature control [23], light control [24], [25] and magnetic control [26]. Among these methods, electrical methods stand out as cost-effective, easily integrable, and controllable approaches. In the microwave band, commonly used electrical diodes include PIN diodes and varactors.

Considering that EM information is discrete and digital, the corresponding tuning mechanism is specifically referred to as a digital switch. These digital switches produce discrete states of the elements, which can be characterized as bits in the physical world. In contrast to general tunable materials, digital switches are inherently compatible with digital information. Consequently, R-MTSs utilizing digital switches, particularly PIN diodes, have garnered significant research attention in recent years. Accordingly, this review focuses on 1-bit and 2-bit R-MTS elements, which are mainly controlled by PIN diodes.

III. 1-Bit Elements

In this section, 1-bit reconfigurable elements that have a single independent switch are reviewed. Due to their 1-bit nature, each element is limited to two states. Consequently, a 1-bit element can manipulate either one dimension of the EM wave or a combination of associated dimensions with only 1-bit information.

Considering that there are five dimensions of EM waves, there are five distinct types of information bit allocation, namely, phase-only, amplitude-only, polarization-only, direction-only and frequency-only elements shown in Figure 2. Over the past decades, researchers have dedicated significant efforts to designing each type of reconfigurable element, leading to notable advances in the field. Some typical achievements of these works are reviewed below.
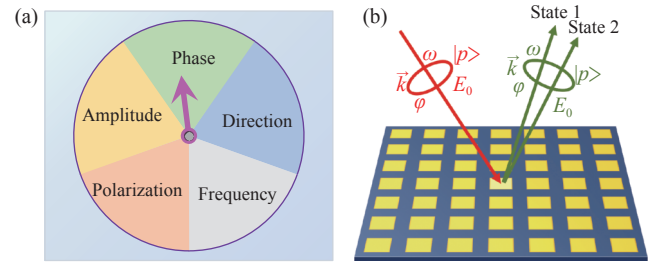
Figure 2 An illustration of 1-bit allocation. (a) One bit of information can be allocated to one of five dimensions at a time, resulting in five types of 1-bit elements. (b) The function of 1-bit reconfigurable elements is shown, where an element can manipulate one incident wave with two different scattering states.

1. Phase-only elements

Phase-only elements are extensively studied among the five types of 1-bit R-MTSs. For phase-only elements, formula (2) is simplified as

$$\vec{E}^{\text{sca}}(\vec{r},t) = \sum_{i=1}^{M} \vec{C}_i(\vec{r}) e^{j(-\vec{k}\cdot(\vec{r}-\vec{r_i})+\Delta\varphi_i(R_i)+\varphi_i^{\text{inc}})} \cdot e^{j\omega t} \qquad (7)$$

where the time-invariant coefficient term is given by

$$\vec{C}_i(\vec{r}) = L_i(\vec{r})A_i E_{0i}^{\text{inc}} F_i(\vec{r}) \mathbb{J}_i |p_i^{\text{inc}}\rangle \qquad (8)$$

Phase-only elements only manipulate the ith additional phase $\Delta\varphi_i$, and the other dimensions are usually invariant with switch configurations and time. Formula (7) indicates that the radiation pattern of the R-MTS is determined by the $\Delta\varphi$ of each element, implying that the near-field phase influences the far-field beam patterns. Phase-only R-MTSs have various applications, such as dynamic beamforming and beam scanning [16], reconfigurable OAM beam generation [19], and reconfigurable holograms [27].

The concept of a 1-bit phase refers to the quantization of a continuous phase into only two phase states. In the design of 1-bit phase elements, researchers typically choose

phase differences between two configurations that are close to 180°. This choice minimizes the phase quantization loss to approximately 3–3.9 dB [28], [29].

Various configurations of 1-bit phase elements have been developed, by employing different configurations, switches, frequency bands and functions. According to the reflectarray theory, additional phases of elements can be tuned by time-delay lines, variable sizes or variable rotating angles [1], [20], [30]. By using the ON and OFF states of RF switches on the elements, one can emulate size changes or angle rotations, thereby altering the additional phase of the elements.

1) Basic phase-only element

In the microwave band, a single PIN diode switch is commonly used to achieve 1-bit phase reconfiguration for single-polarization EM waves [13], [16], [17], [31]–[35]. In [16], [31], [32], independently addressable reconfigurable reflectarray antennas (RRAs) with high efficiency are realized by carefully designing the elements, switches and bias lines (Figure 3(a)). Furthermore, researchers have explored various RRAs operating in different frequency bands. In the millimeter-wave band, a 60-GHz RRA prototype using commercial PIN diodes has been fabricated [33]. Wideband RRAs have also been a focus of research, with a reported bandwidth of up to 38.4% in recent works [35]. In the THz and optical bands, similar modulation principles apply. However, the development in this research field is limited by the immaturity of tunable devices. In recent years, there have been efforts to introduce various tunable materials for phase tuning in these high-frequency bands, which are discussed in Section V.2.

A single control signal with two states used to manipulate multiple switches synchronously is also classified as a 1-bit element. This approach allows for the integration of additional functions into a single element by employing a greater number of associated switches.

2) Phase-only element related with polarization dimension

Stable 180° phase modulation in an entire frequency range and polarization conversion can be achieved by incorporating multiple associated switches. By appropriately designing the elements and switches, a Jones matrix with polarization conversion capabilities can be derived as

$$\mathbb{J} = \begin{bmatrix} 0 & 1 \\ 1 & 0 \end{bmatrix} \tag{9}$$

This Jones matrix can swap the incident polarization; in other words, the reflected polarization is rotated by 90°. By employing a control signal to alternate between the ON and OFF states of the switches, precise 180° phase differences can be achieved. Extensive research has been conducted on the application of polarization conversion principles in the design of RRAs [36]–[40]. For instance, reference [36] demonstrates that alternately switching two PIN diodes controlled by one signal line can achieve a stable 180° reflection phase difference based on the principle of polar-

ization conversion (Figure 3(b)), which can manipulate circular polarization (CP) waves with low design complexity and low insertion loss.

Dual-switch elements can respond to dual-LP and dual-CP waves. In a related study [41], it was reported that a patch with two associated switches positioned on orthogonal sides enables phase tuning with responses to dual-linear and dual-circular polarizations from 13.5 to 15 GHz (see Figure 3(c)).

3) Phase-only element related with direction dimension

In addition to reflective metasurfaces, extensive research has been conducted on transmissive metasurfaces, known as reconfigurable transmitarray antennas (RTAs). It has been proven that a minimum of two switches is needed to construct high-performance 1-bit RTA elements [42]. When designing RTAs, the current reversal method using two switches has proven to be a valuable approach for 1-bit phase control [43]–[49]. For example, a receive–transmit structure in the X band employing two PIN diodes that alter the element configuration is proposed in [43]. By mutually reversing the current by 180°, the transmitted phases are correspondingly reversed by 180° (Figure 3(d)). In contrast to single-layer RTAs with all switches on a single layer, multilayer RTAs with switches distributed across different layers have been proposed in recent years [48], [50], [51]. For instance, reference [51] presented a dual-layer Huygens' element with two associated switches loaded on each layer, enabling 1-bit transmission phase control at 13 GHz (Figure 3(e)).

Furthermore, single-layer R-MTS can facilitate bidirectional beam scanning functions combined with polarization conversion [52]. This configuration, operating in the C band, splits the energy, reflecting half and transmitting the other half (Figure 3(f)).

2. Amplitude-only elements

According to formula (5), the amplitude modulation of an element can be represented by a parameter A. When an EM wave interacts with an MTS, the energy can be amplified ($A > 1$), attenuated ($A < 1$) or maintained ($A \approx 1$). Accordingly, the amplitude-only element can be active, lossy or nearly transparent. Amplitude modulation elements have applications in channel modulation [53], relay amplifying [54] and so on. Several prototypes of microwave band 1-bit amplitude R-MTSs have been demonstrated [54]–[64].

Amplifying transmitarrays based on receive–transmit structures, utilizing active transistors as energy amplifiers, were proposed in the 1990s [55]–[57]. As Figure 3(g) illustrates, a pair of vertical gate leads receives the energy from free space, and two transistors form a differential amplifier with their sources connected [57]. The gate energy is amplified and radiated horizontally by a pair of drain leads. The amplifying/maintaining states can be switched by controlling the ON/OFF states of the power source of the transistors.

An amplifying reflectarray based on FET transistors
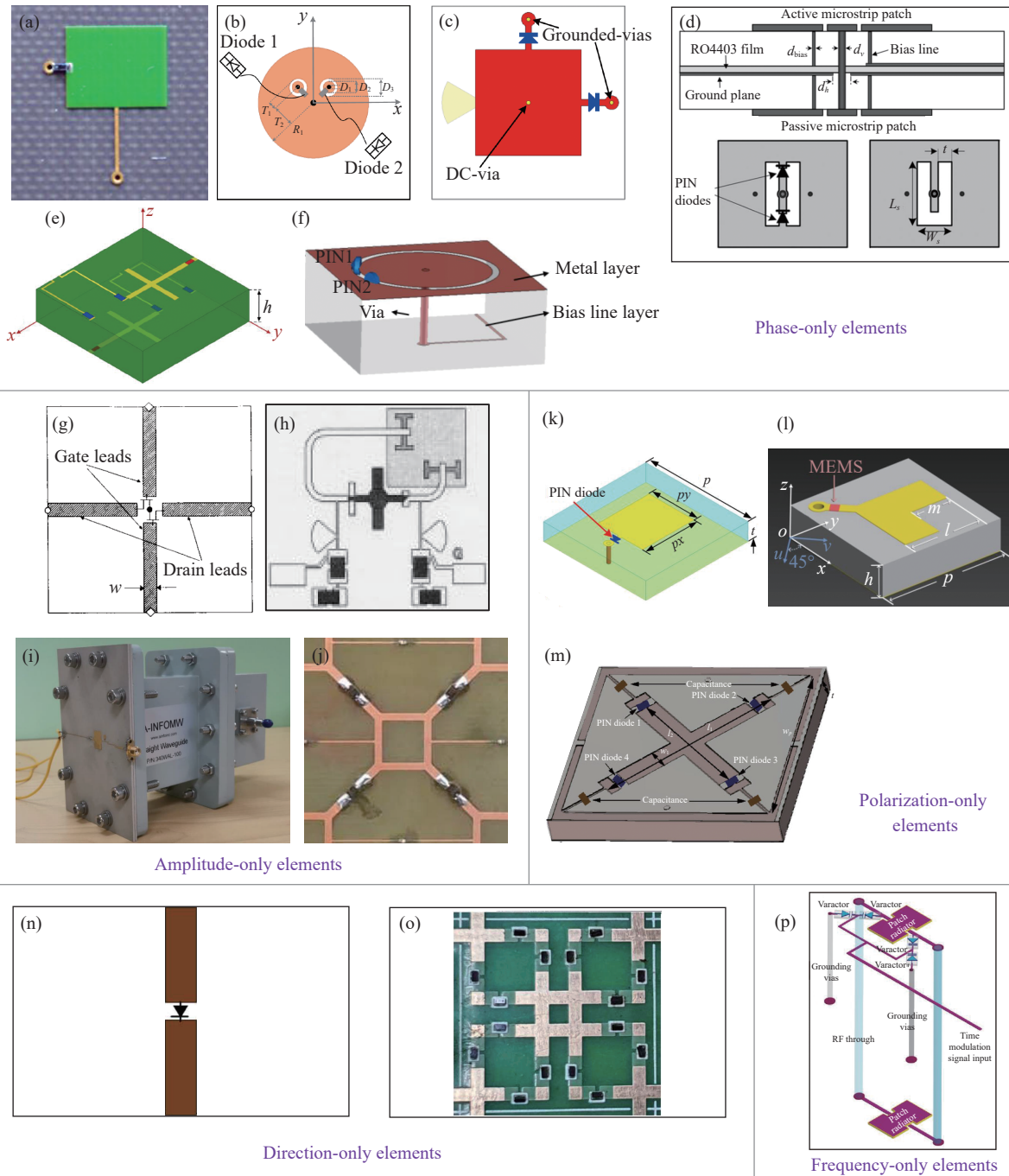
Figure 3 1-Bit reconfigurable elements manipulating one of five dimensions. (a)–(f) Phase-only elements. (a) 1-Bit phase reconfiguration with a single switch on each element [31]. (b) 1-Bit phase reconfigurable reflective element with two switches enabling polarization conversion [36]. (c) 1-Bit element with two switches controlled by one bias signal responding to dual LPs and CPs [41]. (d) Reconfigurable transmitarray element based on the receive–transmit structure. Two PIN diodes are turned ON and OFF alternately, leading to a 180° current reversal on the transmitting structure [43]. (e) Dual-layer reconfigurable transmitarray element with one switch on one layer to tune the phase simultaneously [51]. (f) Single-layer bidirectional re-configurable element [52]. (g)–(j) Amplitude-only elements. (g) Amplifying grid array based on a differential amplifier [57]. (h) Amplifying reflectarray based on FET transistors [58]. (i) Amplifying element using the principle of parametric amplification [59]. (j) Switchable absorbers with four PIN diodes in different directions that have the ability to respond to full polarization [64]. (k)–(m) Polarization-only elements. (k) LP-LP switching element [16]. (l) LP-CP switching element [65]. (m) CP-CP switching element [66]. (n)–(o) Direction-only elements. (n) Cylindrical active dipole elements on an FSS [67]. (o) Complementary #-shaped 1-bit reconfigurable planar FSS for full polarization [68]. (p) Frequency-conversion element based on time modulation [69].

was proposed in [58], as shown in Figure 3(h). The patch receives an LP wave and couples the energy into a mi-crostrip line through an H-shaped slot. The energy is then amplified in the circuit and reradiates into free space through the patch in an orthogonal polarization. The gain is over 10 dB.

Recently, an amplifying reflectarray element based on a parametric amplifier was investigated in [54], [59]. A 2.36

GHz incident signal was amplified and reflected using the nonlinear effect of a varactor on the circuit, with energy provided by a 4.72 GHz pump (Figure 3(i)). The amplifying gain could be tuned by adjusting the pump energy, enabling amplitude reconfiguration.

Switchable absorber–reflectors or absorber–transmitters based on active-frequency selective surfaces (AFSSs) have been developed in recent years [60]–[64], [70]. Imperfect PIN diodes with a large insertion loss in the ON state can absorb energy at the resonance frequency, while in the OFF state, the wave is scattered by the R-MTS without attenuation. Modulating the ON/OFF states allows for amplitude modulation. Elements can respond to multiple polarizations by incorporating several PIN diodes, ranging from LP [61], [62] and dual-LP [63] to full polarizations (Figure 3(j)) [64], [70].

3. Polarization-only elements

Polarization $|p\rangle$ is one of the intrinsic dimensions of spatial EM waves. A 1-bit polarization reconfigurable element switches between two polarization states, which can be mathematically represented by a Jones matrix $\mathbb{J}$ that transitions between the two forms. Furthermore, polarization bits can be utilized for transmitting information [71].

Here, we provide a review of the principle of 1-bit polarization reconfiguration. Suppose the incident polarization is along the x axis. A switch is loaded along the x' axis, where the x'-y' coordinate system is rotated by 45° from the x-y coordinate system, as shown in Figure 4. We consider the scattering responses along the x' and y' axes to be isolated. If the additional phase along the y' axis is $\varphi_{y'}$ and the phase along the x' axis is $\varphi_{x'}$, the element modulation matrix, under the x'-y' coordinate system, can be simply expressed as

$$\mathbb{M}' = \begin{bmatrix} e^{j\varphi_{x'}} & 0 \\ 0 & e^{j\varphi_{y'}} \end{bmatrix} \tag{10}$$

and the incident wave is

$$|p'\rangle = \frac{1}{\sqrt{2}} \begin{pmatrix} 1 \\ 1 \end{pmatrix} \tag{11}$$

Hence, the scattered wave is

$$\vec{E}' = \mathbb{M}'|p'\rangle = \frac{1}{\sqrt{2}} \begin{pmatrix} e^{j\varphi_{x'}} \\ e^{j\varphi_{y'}} \end{pmatrix} \tag{12}$$

Under the x-y coordinate system, the scattered wave is

$$\vec{E} = \frac{1}{2} \begin{pmatrix} e^{j\varphi_{x'}} + e^{j\varphi_{y'}} \\ e^{j\varphi_{x'}} - e^{j\varphi_{y'}} \end{pmatrix} \tag{13}$$

Since the phase along y' is fixed, suppose $\varphi_{y'}$ is fixed at 180°, and the phase along x' is reconfigurable. Let us consider three special cases. (1) $\varphi_{x'}^{ON} = 180°$ and $\varphi_{x'}^{OFF} = 0°$. According to (13), the scattered wave switches between LP(x) and LP(y). (2) $\varphi_{x'}^{ON} = 90°$ and $\varphi_{x'}^{OFF} = 0°$. $\vec{E}^{ON}$ yields
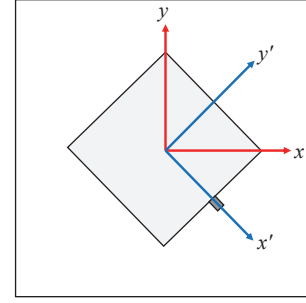
Figure 4 Illustration of coordinate system definitions considering polarization.

circular polarization, and $\vec{E}^{OFF}$ yields linear polarization. Hence, polarization modulation between LP and CP waves is obtained. (3) $\varphi_{x'}^{ON} = 90°$ and $\varphi_{x'}^{OFF} = -90°$. The scattered waves correspond to two spins of CP. Hence, a dual-CP transition can also be generated and switched. This discussion is summarized in Table 1.

Table 1 A summary of 1-bit polarization manipulation types

$\varphi_{y'} = 180°$	Incident polarization	Scattered polarization
$\varphi_{x'}^{ON} = 180°$ $\varphi_{x'}^{OFF} = 0°$	LP(x)	LP(x)-LP(y)
	CP	RHCP-LHCP
$\varphi_{x'}^{ON} = 90°$ $\varphi_{x'}^{OFF} = 0°$	LP(x)	LP-CP
	CP	
$\varphi_{x'}^{ON} = 90°$ $\varphi_{x'}^{OFF} = -90°$	LP(x)	RHCP-LHCP
	CP	LP(x)-LP(y)

Various prototypes have been developed to verify the transitions of LP(x)-LP(y), LP-CP and LHCP-RHCP, as described in [16], [65], [66], [72]–[75]. LP-LP switching based on a transmitarray was investigated in [16], [74], [75], where the ON/OFF states of PIN diodes were tuned to convert or maintain the linear polarization of the reflected wave (Figure 3(k)). The conversion between LP and CP is studied in [65] using LP incidence (Figure 3(l)). When the switch is ON, a phase difference of 180° is achieved along the x' and y' axes, resulting in polarization conversion. When the switch is OFF, a phase difference of 90° is obtained, leading to the generation and reflection of CP. Additionally, polarization-only R-MTSs can dynamically convert LP incident waves to RHCP or LHCP [66] by modulating the phase difference between the x' and y' axes to 90° or −90° (Figure 3(m)). Other states of polarizations can also be switched, as summarized in Table 1.

4. Direction-only elements

In formula (5), F denotes the element radiation pattern, which determines the direction of the main beam scattered by a single element. It is worth mentioning that the element radiation pattern is not equivalent to the array radiation pattern. The array radiation pattern takes into account not only the element radiation pattern but also other element properties, such as phase and amplitude, as derived in (7) and (8). Here, we only investigate radiation pattern reconfiguration

at the element level.

Reflection–transmission pattern reconfigurable AFSSs have been comprehensively studied in recent years [67], [68], [75]–[77]. For example, a dipole FSS with tunable PIN diodes at the center was reported in [67], which enables the switching of the reflection/transmission states of the EM wave from 2.3 GHz to 3 GHz (Figure 3(n)). When the PIN diode is in the ON state, the dipole is resonant, which can block the EM wave and cause reflection. Conversely, when the PIN diode is in the OFF state, the dipole is not excited, allowing the EM wave to pass through the FSS. Furthermore, elements with complementary reflection and transmission responses in full polarization were reported in [68], as shown in Figure 3(o). The #-shaped AFSS element can create complementary stop/pass bands and is capable of responding to full polarizations.

It is worth noting that $\vec{k}$ represents a vector in the entire space, indicating propagation in various directions, not only forward or backward. Direction-only vector types include propagation at different angles based on pattern reconfiguration. While reflection- and transmission-type direction reconfigurable elements have been well studied, to the best of our knowledge, direction-only elements specifically dedicated to pattern reconfiguration on one side (angle reconfiguration) have not been reported in the published literature. More research in this area can be anticipated in the future.

5. Frequency-only elements

Converting frequency is crucial in communication applications. The inherent operating mechanism of generating new frequencies is the nonlinear effect. Therefore, the EM elements used in frequency conversion should possess nonlinear characteristics. The concept of frequency-only R-MTSs has been explored since the 1980s [78]. However, due to the complexity of the elements and the limited practical applications, this area of research has received relatively little attention in the past few decades. Recently, with the rapid development of digital control circuits such as field programmable gate arrays (FPGAs), utilizing the time dimension to generate new frequencies based on R-MTS has become feasible [69], [79]–[82]. Figure 3(p) illustrates a frequency-conversion element capable of mixing the frequencies of spatial EM waves and guided waves and subsequently reradiating the mixed wave into free space, which can introduce more than a 1-GHz frequency shift [69].

Here, we briefly introduce the principle of frequency generation based on the time modulation technique. In (4), the notation R indicates the reconfiguration of the element as a function of time t. Let us consider a phase-only element that is subjected to a periodic control signal with a period T. As a result, the additional phase of the element can be modulated periodically. According to (5), and considering that the only variable is the phase ($\Delta\varphi$), the main term of the element modulation function is

$$M(t) = e^{j\Delta\varphi(t)} \tag{14}$$

$M(t)$ is also a periodic function of time t. Applying the Fourier expansion, $M(t)$ is expressed as

$$M(t) = \sum_{h=-\infty}^{\infty} a_h e^{j\frac{2\pi h}{T}t} \tag{15}$$

where $\{a_h\}$ is a Fourier series and

$$a_h = \frac{1}{T}\int_{-\frac{T}{2}}^{\frac{T}{2}} e^{j\Delta\varphi(t)} e^{-j\frac{2\pi h}{T}t}\mathrm{d}t \tag{16}$$

Harmonic frequency components are generated when $\Delta\varphi(t)$ is not a constant value. According to (2), when the incident frequency is f_c, the core term of the scattered wave is

$$E(t) = \sum_{h=-\infty}^{\infty} a_h e^{j(2\pi f_c + \frac{2\pi h}{T})t} \tag{17}$$

As formula (17) illustrates, new frequencies are added to the incident frequency, and the harmonic frequency components of the spatial wave are reconfigurable if the control signal or the switching period is adjustable.

In essence, the EM element acts as a frequency mixer by combining the frequency in free space with the switching frequency of the FPGA on board. The reason why rapidly switching elements can act as a mixer is that the lumped switch is a nonlinear component. By modulating the ON/OFF states of the switch over time, a square-wave phase is generated, which serves as the inherent source of new frequency generation. We note that the maximum frequency shift is determined by the switching speed of the switches and the FPGA, which is currently much lower than the frequency of the spatial EM wave ($1/T \ll f_c$). Therefore, there is still room for improvement in terms of achieving significant frequency shifts through the rapid switching of states in elements.

IV. 2-Bit Elements

This section reviews the advances in 2-bit elements with two independent switches. By incorporating more information bits into a single element, the R-MTS becomes multidimensional, enabling the realization of various functions.

Note that the response notation R in (4) is determined by two components: *control* and *excitation*. Following the information allocation strategy, there are two types of allocation for 2 bits: both bits go to *control*, or one bit is allocated to *control* and the other bit is allocated to *excitation*.

In the first type, each element can actively manipulate 2 bits of information simultaneously, which is referred to as the 2-bit manipulation type. Since there are five dimensions of the EM wave, the 2 bits can be allocated to these five dimensions individually, as shown in Figure 5(a). There are C_5^2 ways to allocate the 2 bits to two different dimensions and 5 ways to allocate both bits to a single dimension. Thus, there are a total of $C_5^2 + 5 = 15$ ways to allocate the 2 bits for the 2-bit-manipulation type elements.
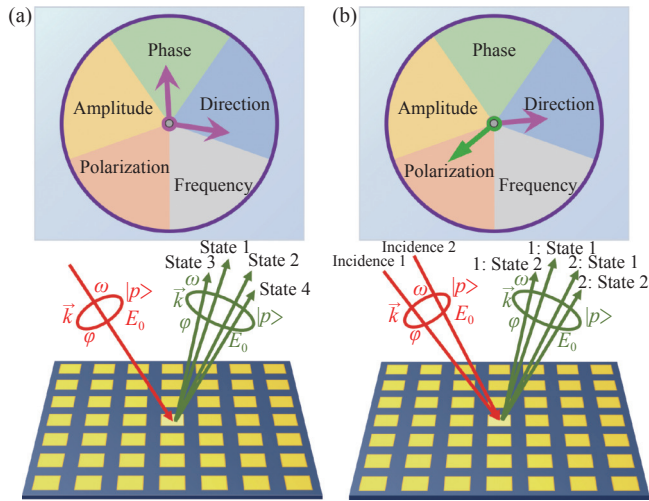
Figure 5 Illustrations of two types of 2-bit allocation. (a) 2-Bit-manipulating type: This type allows for the active manipulation of one or two dimensions under one incident wave. The figure shows two bits allocated to five dimensions. This results in a total of $C_5^2 + 5 = 15$ combinations for this type of bit allocation. (b) Multiplexed–manipulating type: This type enables the manipulation of one dimension (represented by the pink arrow) while responding to two incident waves that differ in one dimension (represented by the green arrow). The figure illustrates that there are theoretically $5 \times 5 = 25$ ways of performing bit allocation for this type.

In the second type, the element can be designed to actively control 1 bit of information in one dimension while independently responding to the excitations of two incident waves in one dimension using the other bit. By multiplexing one element, two incident waves can be manipulated independently, so we call these elements multiplexed-manipulating type elements. Theoretically, there are $5 \times 5 = 25$ combinations of this type, as illustrated in Figure 5(b).

Here, some existing combinations are reviewed, and the others need to be further studied.

1. 2-Bit-manipulating type element in one dimension

1) 2-Bit-phase reconfigurable element

The 2-bit-phase element, where both bits are allocated to the phase dimension, has been widely studied [83]–[88]. Such elements offer four relative phase states, 0°, 90°, 180°, and 270°, thereby improving phase resolution and reducing quantization loss compared to the 1-bit phase by approximately 2.4–3 dB [28], [29].

For 2-bit phase modulation, a minimum of two switches is needed. Both reflective and transmissive 2-bit-phase R-MTSs are realized. In reference [83], a reflective asymmetric pentagon-shaped element based on the resonance method was proposed (Figure 6(a)), capable of generating four reflection phase states at approximately 7 GHz. For 2-bit-phase transmitarrays, additional switches are employed in receive–transmit structure-based transmitarrays [85]. The receiving patch achieves a 0°/180° phase shift, while the transmitting structure achieves a 0°/90° phase shift, enabling the generation of four phase states (Figure 6(b)).

2) 2-Bit-amplitude reconfigurable element

A 2-bit-amplitude R-MTS, capable of amplifying,

maintaining, and attenuating amplitude, is realized by controlling the supply voltages of two amplifiers on each side of a receive–transmit structure-based transmitarray [89], as shown in Figure 6(c). It can realize four distinct amplification levels (−10 dB, 0 dB, 10 dB, 20 dB). Notably, continuous amplitude reconfiguration can also be achieved by continuously tuning the supply voltages.

3) 2-Bit-polarization reconfigurable element

2-Bit-polarization reconfigurable elements have also been reported in recent literature. These elements actively generate and modulate three polarization states using two independent switches [90]. PIN diodes are soldered along the x and y axes (Figure 6(d)), with a 90° ON/OFF phase difference along the two axes. As a result, 90°, −90°, and 0° phase differences between the x and y axes can be achieved by independently tuning the two switches. When the incident LP polarization is along the x' axis, RHCP, LHCP, and LP reflection waves are obtained. It is worth noting that the unused state among the four states is the 90° phase of LP.

Furthermore, we propose two approaches to achieving a four-state polarization reconfiguration: RHCP, LHCP, LP(x'), and LP(y'). First, if the incident polarization is along the x' axis, the desired polarization states can be obtained by setting the additional phase to 0°/180° along the x axis and 0°/90° along the y axis. The second approach involves fixing the reflection phase along the y axis, such as 180°. In this case, a 2-bit-phase reconfigurable element with a tunable phase along the x axis can also function as a 2-bit-polarization reconfigurable element when the incident polarization is along the x' axis.

4) 2-Bit-frequency reconfigurable element

Frequency reconfigurable elements are typically constructed through time modulation, which is discussed in Section IV.3.

2. 2-Bit-manipulating type elements in two different dimensions

1) Phase-amplitude reconfigurable element

A phase-amplitude reconfigurable element allocates one bit to phase and the other bit to amplitude control. This type has found applications in generating modulation signals and reducing the sidelobe levels of beam patterns. In [91], a dual-layer structure was presented where the top layer, made of graphene, manipulates the reflection amplitude, while the bottom layer, consisting of PIN diodes, tunes the reflection phase. In [92], single-layer elements integrated with two types of PIN diodes were proposed (Figure 6(e)). Here, one PIN diode is designed to have minimal insertion loss in the ON state and high isolation in the OFF state, allowing for phase tuning while maintaining the reflection amplitude. The other PIN diode exhibits minimal insertion loss in the ON state and absorbs a large portion of energy in the OFF state without significantly affecting the phase. These carefully designed configurations enable the realization of a 2-bit phase-amplitude reconfigurable element.

An energy-amplifying reflectarray that modulates the reflection phase was proposed in reference [93], as shown
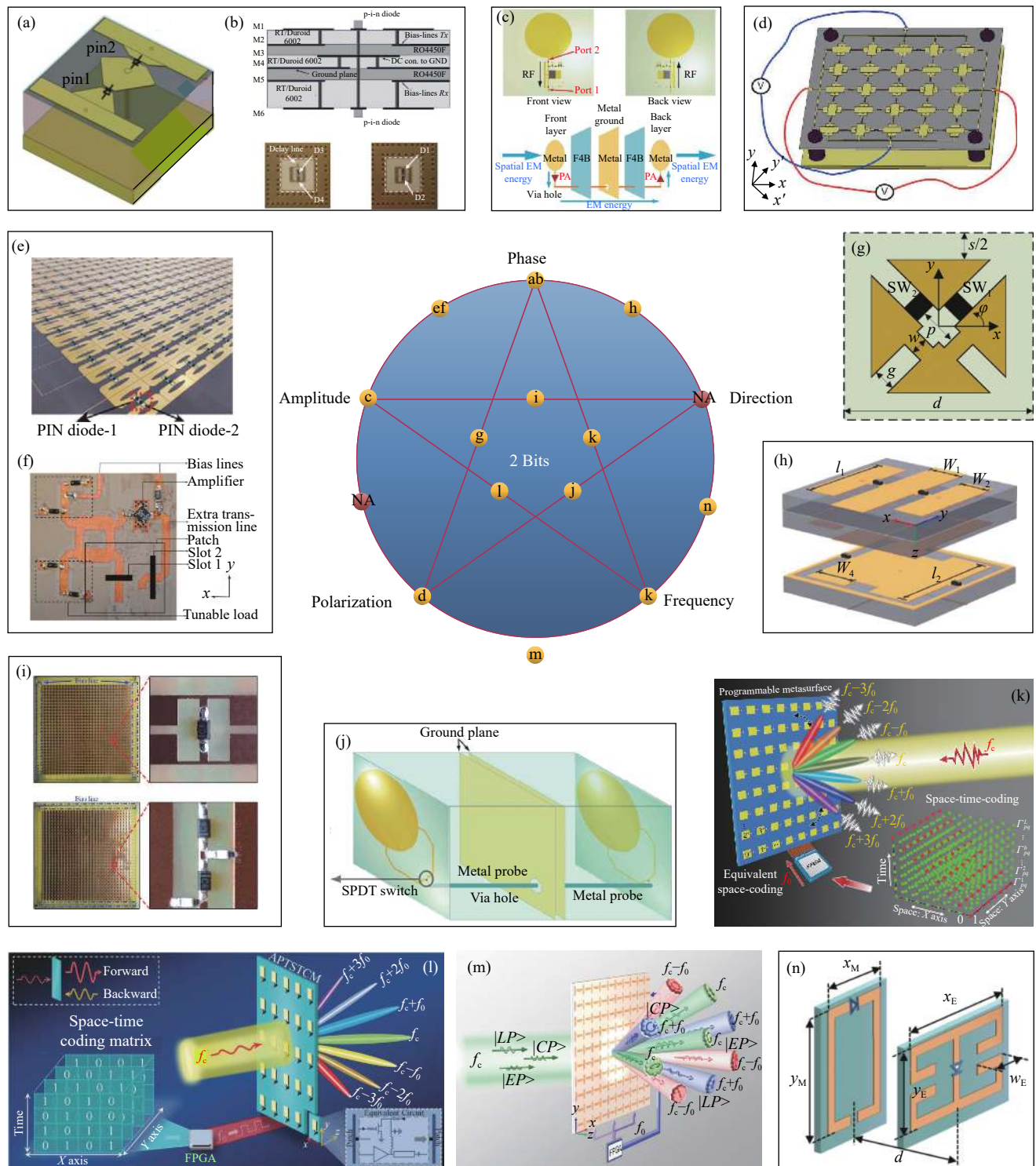
Figure 6 2-Bit reconfigurable elements actively manipulating one or two of five dimensions. (a) 2-Bit-phase reconfigurable reflectarray based on four switchable resonant states [83]. (b) 2-Bit-phase reconfigurable transmitarray based on a receive–transmit structure with two sets of switches on each side [85]. (c) 2-Bit-amplitude reconfigurable element realizing amplitude amplification, maintenance and attenuation functions [89]. (d) 2-Bit-polarization R-MTS with the ability to switch among RHCP, LHCP and LP states [90]. (e) Phase-amplitude R-MTS with one PIN diode modulating the phase and the other controlling whether the amplitude is attenuated [92]. (f) Phase-amplitude reconfigurable reflective element with a varactor tuning the phase and a transistor controlling the amplitude [93]. (g) Phase-polarization reconfigurable element with two independent switches operating synchronously [95]. (h) Phase-direction reconfigurable element with two PIN diodes modulating the phase and two PIN diodes manipulating the direction [99]. (i) Direction-amplitude reconfigurable prototype [101]. (j) Direction-polarization reconfigurable element using two SPDT switches [102]. (k) Illustration of frequency or frequency-phase reconfiguration [103]. (l) Frequency-amplitude R-MTS, where the amplification level is tunable at harmonic frequencies based on space-time modulation [104]. (m) Frequency-polarization reconfiguration based on a time modulation strategy. [105]. (n) Frequency-direction reconfigurable Huygens element based on dynamic space-time modulation [106].

in Figure 6(f). A patch and an I-shaped slot convert the y-polarized spatial wave into a guided wave. Varactors are incorporated along the transmission line for phase modulation, while a lumped amplifier amplifies the energy on the transmission line. Finally, the energy is reradiated as an x-polarized wave through the slot and patch.

2) Phase-polarization reconfigurable element

Phase-polarization reconfigurable elements can enable beam alignment and polarization synchronization applications. In 2010, reference [94] introduced the concept of simultaneously achieving phase modulation and polarization control in reflectarrays. This was accomplished using a dual-polarized reconfigurable element (we classify it as a polarization-multiplexed phase-manipulating type in Section IV.4.2)). When the incident polarization is along the x' axis, the lossless modulation matrix of the dual-polarized reconfigurable element in the x-y coordinate system is expressed as

$$\mathbb{M} = \left[\begin{array}{cc} e^{j\varphi_x} & 0 \\ 0 & e^{j\varphi_y} \end{array} \right] \tag{18}$$

Following a similar derivation to that of (11)–(13), the reflection wave in the x'-y' coordinate system is

$$\vec{E'} = \frac{1}{2} \left(\begin{array}{c} e^{j\varphi_x} + e^{j\varphi_y} \\ e^{j\varphi_x} - e^{j\varphi_y} \end{array} \right) \tag{19}$$

with a 1-bit reconfigurable phase along the x and y axes independently. Suppose the phases switch between 0°/180° in the OFF and ON states; then, the four states of the reflection wave are obtained as follows:

$$\vec{E'}_{\text{ON--ON}} = \left(\begin{array}{c} e^{j180°} \\ 0 \end{array} \right), \vec{E'}_{\text{OFF--OFF}} = \left(\begin{array}{c} e^{j0°} \\ 0 \end{array} \right) \\ \vec{E'}_{\text{OFF--ON}} = \left(\begin{array}{c} 0 \\ e^{j0°} \end{array} \right), \vec{E'}_{\text{ON--OFF}} = \left(\begin{array}{c} 0 \\ e^{j180°} \end{array} \right) \tag{20}$$

As this demonstrates, polarization switches dynamically between the x' and y' axes, with independent modulation of the reflection phase.

As shown in Figure 6(g), a simplified reflective element with 2-bit phase-polarization reconfiguration was further designed and simulated in [95]. Additionally, in recent years, RTAs based on receive–transmit structures have demonstrated the capability of 2-bit phase-polarization modulation for transitioning between LP(x) and LP(y) [96]. Furthermore, by designing the phase difference along the x' and y' axes as 90°/−90°, it is possible to generate and modulate RHCP/LHCP, as demonstrated in [97].

3) Phase-direction reconfigurable element

The phase-direction reconfigurable element is a recently emerging type [98]–[100]. An example of such an element is illustrated in Figure 6(h), consisting of two layers where the top layer controls the phase and the bottom layer controls the direction. Each element can be independently controlled using 1 bit for phase reconfiguration and 1 bit for direction reconfiguration. This type can be used to achieve

signal coverage of the full space.

4) Direction-amplitude reconfigurable element

The direction-amplitude manipulation type is another configuration of 2-bit elements used for reflection, transmission, or absorption switching applications [101], [107]. In [101], a structure with two layers of substrate soldered with PIN diodes was proposed (Figure 6(i)). PIN diodes on the top layer determine whether the EM wave passes through the first layer or is absorbed, while the PIN diodes on the bottom layer control the reflection or transmission states. Note that this configuration has only three states for a 2-bit element. This is because when the EM energy is absorbed on the top layer, the propagation directions of the EM wave become irrelevant.

5) Direction-polarization reconfigurable element

The direction-polarization reconfigurable element was reported in a recent study [102]. It involves a reflecting–transmitting R-MTS controlled by incident polarization. The design includes two identical structures on the top and bottom layers, each equipped with a single-pole double-throw (SPDT) switch (Figure 6(j)). The top SPDT switch determines which polarization state can be transmitted to the bottom layer, while the bottom SPDT switch controls the polarization state of the transmitting wave. Consequently, when the incident polarization is along the x axis, three states can be obtained: an x-polarized reflection wave, x-polarized transmission wave, and y-polarized transmission wave, allowing independent manipulation of polarization and direction.

3. 2-Bit-manipulating type elements related to frequency reconfiguration

Frequency reconfiguration was discussed in Section III.5. Here, the manipulation of frequency, along with other dimensions of the EM wave, is achieved by leveraging the properties of control signals. According to (16), the complex number a_h represents the amplitude and phase responses of the hth harmonic frequency, which are determined by the time series of the control signal. Each a_h can be tailored with considerable flexibility. Consequently, diverse wave dimensions at harmonic frequencies can be independently modulated by employing distinct switchable control signal series. In particular, the time-modulation strategy can be used to design 2-bit-manipulating type elements related to frequency reconfiguration.

1) 2-Bit-frequency and frequency-phase reconfigurable element

References [103]–[111] demonstrated that it is possible to independently modulate phases at different harmonic frequencies using 1-bit or 2-bit phase reconfigurable elements by deliberately designing the time series of the elements. In Figure 6(k), different phase states at different harmonic frequencies can be generated simultaneously (e.g., φ_1 and φ_2 at f_1, φ_3 and φ_4 at f_2), so this is a phase-frequency reconfigurable type. Furthermore, by adjusting the time modulation period T, the harmonic frequency can be modulated ($f_c \pm k f_0$), thereby achieving frequency reconfigurabil-

ity. Specifically, 2-bit frequency reconfiguration can be realized using this type of element.

2) Frequency-ampitude reconfigurable element

The frequency-amplitude reconfiguration type has also been reported recently [104]. As shown in Figure 6(l), this approach involves the integration of an amplifier and a FET onto a passive structure. Through dynamic control of the FET, the R-MTS can produce tunable amplified EM waves at various harmonic frequencies.

3) Frequency-polarization reconfigurable element

In recent years, significant progress has been made in the field of arbitrary polarization reconfiguration using the time modulation strategy [112], [105]. For example, orthogonal dipoles with two sets of PIN diodes are modulated dynamically, which enables the control of the transmitted amplitude and phase of orthogonal LP waves at harmonic frequencies (Figure 6(m)). By combining these modulated LP waves, it becomes possible to generate arbitrary transmitted polarizations.

4) Frequency-direction reconfigurable element

In reference [106], a frequency-direction reconfiguration element is presented, as illustrated in Figure 6(n). This approach involves the design of a time-varying Huygens' metasurface that enables the control of the energy ratio between reflection and transmission at harmonic frequencies. By employing a space-time modulation strategy, it becomes possible to manipulate the beam scanning angles as well.

5) Discussion

According to the information allocation strategy, a single reconfigurable element with at least N-bit physical devices can modulate N-bit information. Here, the rapid switching of element states enables the incorporation of extra tunable bits through time-domain modulation. Therefore, this type of R-MTS is referred to as a *time-modulated metasurface*. However, when time-invariant elements form a periodic array with distinct states at different element locations, the amount of information is multiplexed through space-domain modulation. This type is the *space-modulated R-MTS*, which corresponds to array-level reconfiguration, as discussed previously. Moreover, the combination of space modulation and time modulation gives rise to *space-time-modulated R-MTSs*, which exploit additional dimensions in both the space and time domains. The integration of space and time modulation enables the realization of novel functions, making this a promising area for the future research.

4. Multiplexed-manipulating type elements

In addition to those that actively manipulate two dimensions, another significant category of 2-bit elements involves manipulating one dimension while independently responding to two different incident waves. The multiplexed-manipulating type theoretically offers 25 combinations, although some are impractical. Here, we review the existing combinations and propose some ideas for unrealized combinations.

1) Frequency-multiplexed phase-manipulating element

Frequency-multiplexed phase control is a natural approach for full duplex communication using a single R-MTS. To independently modulate the phase in response to two frequency bands with the same polarization, one can design a supercell consisting of two independent elements working at two bands in the Ku band [113]–[115], an example of which is shown in Figure 7(a).

2) Polarization-multiplexed phase-manipulating element

Polarization-multiplexed phase manipulation is a well-studied type [116]–[120]. By leveraging the isolation between two orthogonal directions, elements can independently manipulate two polarizations, allowing a single element to operate on two incident waves with orthogonal polarizations simultaneously. As shown in Figure 7(b), a cross-shaped element with two sets of independent MEMSs can modulate the reflection phase of dual-LP waves in the X band [116].

Additionally, a dual-LP-multiplexed transmitarray is demonstrated in [120]. By orthogonally arranging two 1-bit phase-reconfigurable dipoles, the transmitarray achieves polarization multiplexing in the Ku band (Figure 7(c)).

The abovementioned studies focused on LP incidence. We note that there have been studies on fixed metasurfaces for independent dual-CP multiplexing [120]–[124], but independent phase reconfiguration for dual-CP incident waves has not been reported in the literature, making it a potential future research topic.
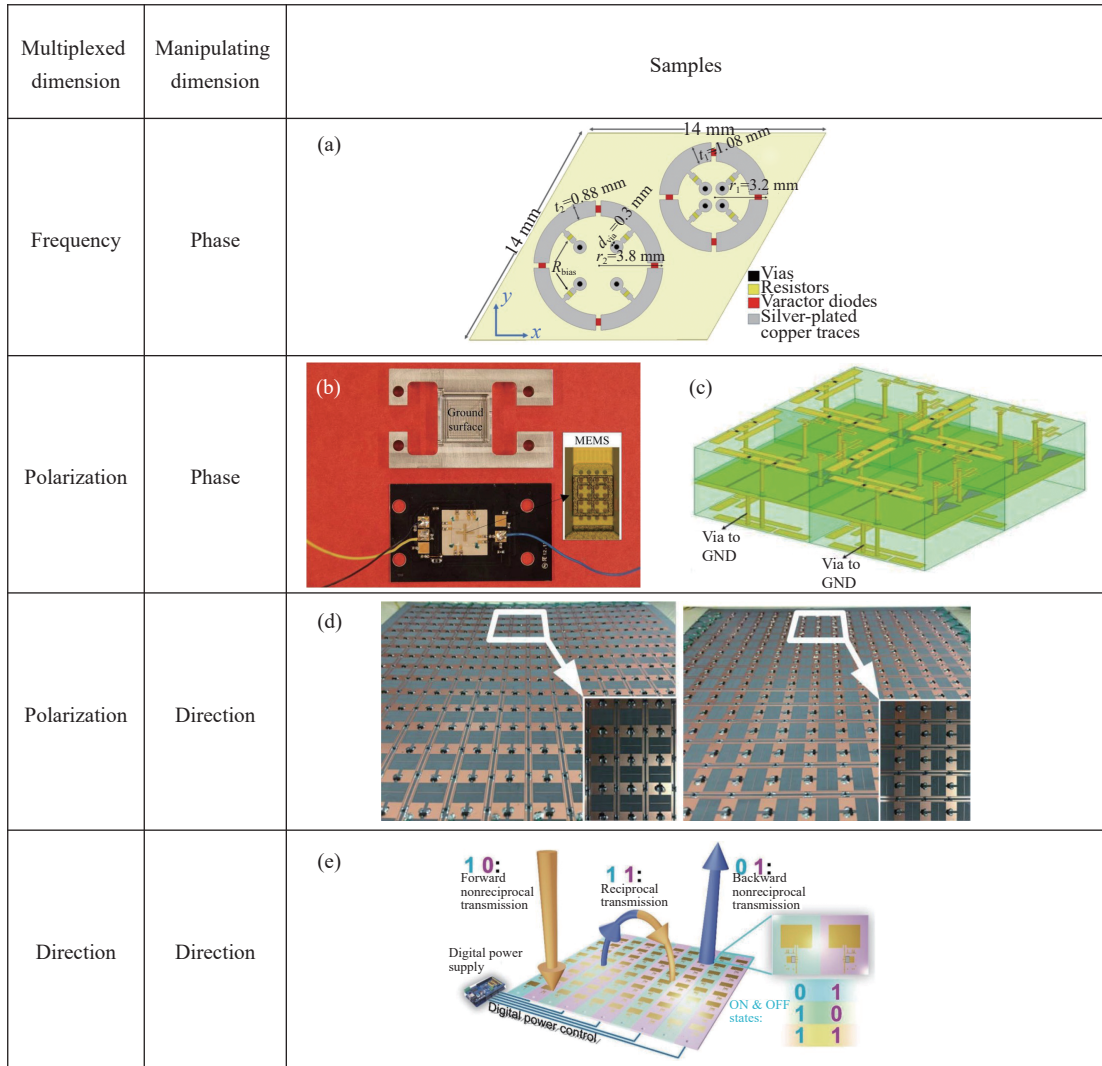
3) Polarization-multiplexed direction-manipulating element

Polarization-multiplexed direction manipulation is an extension of 1-bit direction reconfiguration, as discussed in Section III.4. In [125], [126], orthogonal switches were integrated on two layers to independently manipulate the propagating directions of two incident polarizations. Figure 7(d) provides an example of such a configuration. Moreover, a polarization conversion layer is introduced on top of these layers to enable polarization conversion functionalities [127]. Additionally, fixed-phase layers are incorporated at the top and bottom, allowing the generation of different holographic images in response to different incident polarizations with controllable directions [128].

4) Direction-multiplexed direction-manipulating element

A 2-bit R-MTS capable of modulating the direction of a wave while responding to two incident wave directions was presented in [129]. This design exploits the inherent nonreciprocity of an amplifier to achieve independent direction modulation on both sides. The supercell consists of two opposing amplifying elements that can respond independently to forward and backward waves (Figure 7(e)). When the forward element operates in the ON state, the forward EM energy is amplified and transmitted; otherwise, the forward energy is blocked and reflected backward. The backward element operates in a similar manner to modulate the

Multiplexed dimension	Manipulating dimension	Samples
Frequency	Phase	(a)
Polarization	Phase	(b) (c)
Polarization	Direction	(d)
Direction	Direction	(e)

Figure 7 Two-bit reconfigurable elements with one multiplexed dimension and one manipulating dimension. (a) Frequency-multiplexed phase-manipulating element with two reconfigurable elements in one supercell operating at the two frequency bands [114]. (b) Polarization-multiplexed phase-manipulating reflective element [116]. (c) Polarization-multiplexed phase-manipulating transmitarray [120]. (d) Polarization-multiplexed direction-manipulating prototype [126]. (e) Direction-multiplexed direction-reconfigurable design [129]. The supercell determines whether EM waves from the two sides can pass through the MTS.

direction of the backward-incident EM wave. Consequently, the incident waves from the two directions can be modulated independently.

5) Unrealized multiplexed-manipulating types to be explored

As demonstrated previously, there is growing interest in multifunctional R-MTSs of multiplexed-manipulating types. In the following paragraphs, we discuss some ideas for other types of multiplexed-manipulating reconfigurable elements that have not been realized.

One promising topic is direction-multiplexed phase modulation. There are two types of direction multiplexing to consider. The first type, referred to as the *Janus metasurface* [130], [131], involves a metasurface that responds to bidirectional incident waves independently, resulting in two distinct transmitting holographic images from both sides of the MTS [131].

Furthermore, the term *direction* in this context not only refers to opposite directions but also includes incident angles. Based on this, another type to consider is angle-multiplexed phase modulation, where independent beam patterns are designed to generate different incident angles on the MTS. Angle-sensitive elements were proposed in references [132]–[137] to respond to different incident angles independently.

Direction-multiplexed MTSs are a current research trend, but existing works primarily focus on fixed MTSs. The exploration of reconfigurable direction-multiplexed phase tuning holds great potential for the future.

In addition to direction-multiplexed reconfiguration, polarization-multiplexed reconfiguration is an intriguing topic. While the review above primarily covered phase and direction reconfiguration based on polarization multiplexing, polarization-multiplexed amplitude and frequency reconfiguration remain largely unexplored. Future research could delve into these areas.

V. Emerging Topics and Future Trends

1. *N*-bit elements

This paper mainly reviews 1-bit and 2-bit reconfigurable elements. However, it is worth noting that there is ongoing research on elements with more than 2-bit reconfiguration, which is an area of interest [138], [139]. Following the concepts of 1-bit and 2-bit allocation, Figure 8 provides an illustration of *N*-bit allocation.
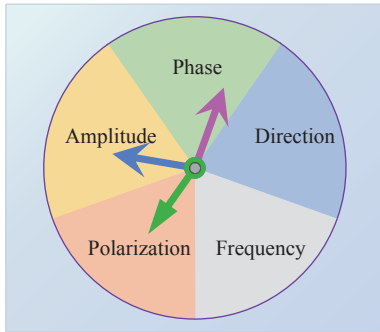
Figure 8 Illustration of *N*-bit allocation. *N* bits can be independently allocated to five dimensions using different combinations of multiplexed and manipulating bits. By linking more dimensions through a single element with higher resolution, the functionality of the R-MTS can be significantly enhanced compared to a 1-bit or 2-bit R-MTS.

Allocating *N* bits to a single dimension can enhance the resolution and improve performance in that dimension. Furthermore, exploring full-dimensional elements capable of modulating all five dimensions of EM waves presents an opportunity to significantly expand the functionalities of R-MTSs, making this a promising area of research. It is worth noting that the quantization loss for 2-bit phase reconfiguration, ranging from 0.6 to 0.9 dB [28], [29], is acceptable in most applications, and similar conditions apply to other dimensions. Therefore, the allocation of *N* bits to diverse dimensions generally offers greater rewards than solely increasing the resolution of a single dimension. In addition, *N*-bit multiplexed-manipulating type R-MTSs are capable of manipulating multidimensional EM waves with a single element.

However, designing elements with reconfigurable dimensions exceeding 2 bits is significantly complex. As discussed in Section III, a 1-bit reconfigurable element can effectively manipulate one of five dimensions independently. Nevertheless, as demonstrated in Section IV, attaining simultaneous and independent control over two dimensions using 2-bit elements presents challenges. In fact, certain 2-bit types remain unrealized. The task of achieving simultaneous and independent control over more than 2 bits introduces even greater difficulties. Various potential approaches exist for the realization of *N*-bit elements. One approach is to integrate additional lumped switches onto a single element. However, due to the bulky size of switches and the complexity of bias lines, the number of switches on a single element is limited. Alternatively, the use of continuously

tunable switches such as varactors can enable multibit reconfiguration. However, this approach requires precise voltage control, which is not robust and introduces complexity from the control circuit. As discussed in Section IV.3, time-modulated MTS holds potential for *N*-bit modulation and multidimensional elements. Nevertheless, challenges such as limited radiation efficiency, complex voltage control requirements, narrow bandwidth, and low modulation speed need to be addressed. Accordingly, the development of multidimensional *N*-bit elements remains a challenging topic for future research.
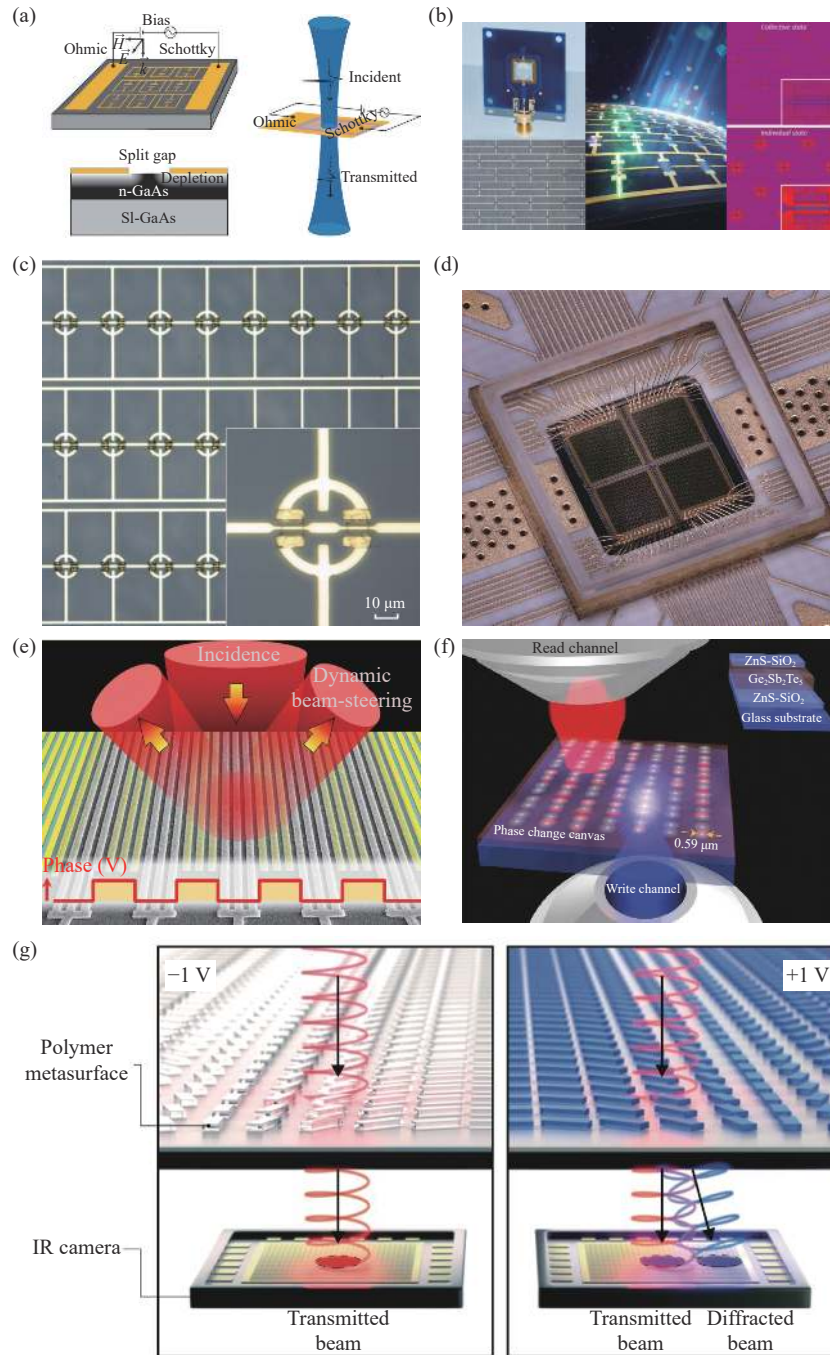
2. Terahertz and optical R-MTSs

In recent decades, microwave band R-MTSs have achieved significant breakthroughs due to the availability of high-performance lumped switches such as PIN diodes and varactors, as well as the maturity and low cost of fabrication processes such as printed circuit board (PCB) technology. There is a growing demand for R-MTSs in the THz and optical bands. However, in these frequency ranges, commercial lumped switches are too large to be effectively utilized, and the ON/OFF ratio is reduced. Therefore, scientists are actively exploring new switches and architectures that can offer higher frequency operation and better performance. With revolutionary advances in micro- and nanofabrication technologies in recent years, R-MTSs in the THz and optical bands are experiencing rapid development.

In the THz band, numerous switches have been introduced, such as Schottky diodes [140], [141] (Figure 9(a)), high-electron-mobility transistors (HEMTs) [142]–[146] (Figure 9(b) and (c)), graphene [147], [148], complementary metal oxide semiconductors (CMOSs) [139], [149], [150] (Figure 9(d)), and vanadium dioxide (VO_2) [151]–[153]. For instance, HEMT switches offer a high ON/OFF ratio and low control complexity, making them suitable for 1-bit phase control in the THz band [142], [143]. Additionally, spatial THz amplitude modulators based on HEMT switches have been reported in [144], [145], demonstrating a 93% amplitude modulation depth and a modulation rate of 1 GHz.

In the optical frequency band, no lumped switches are available. Instead, elements serve as both nanoantennas and switches [154]. These switches are made of materials such as indium tin oxide (ITO) [155] (Figure 9(e)), graphene [156], the chalcogenide compound germanium-antimony-tellurium (GST) [157]–[162] (Figure 9(f)), liquid crystals [163], and the polymer poly(3,4-ethylenedioxythiophene):polystyrene sulfonate (PEDOT:PSS) [164] (Figure 9(g)). For example, phase-change materials such as GST exhibit significant switching performance in the optical band. By inducing the amorphous-crystalline transition of GST using femtosecond pulses, the resonance states of the element can be altered, enabling the modulation of amplitude [157].

However, THz and optical R-MTSs still face several challenges that need to be addressed, such as improving efficiency, increasing switching speed, eliminating grating lobes and achieving independent addressing. Furthermore,

Figure 9 (a)–(d) Terahertz and (e)–(g) optical R-MTSs. (a) Schottky diode-based THz amplitude-reconfigurable array [140]. (b) HEMT-based THz amplitude-reconfigurable transmitarray [145]. (c) HEMT-based THz phase-reconfigurable prototype [143]. (d) CMOS-based THz phase-reconfigurable prototype [139]. (e) ITO-based optical phase-reconfigurable prototype [155]. (f) GST-based optical amplitude-reconfigurable design [157]. (g) PEDOT: PSS-based optical phase-reconfigurable design [164].

the development of multidimensional and multifunctional R-MTSs in the THz and optical bands is an important future direction in this field.

3. Surface-wave R-MTSs

Most of the abovementioned MTSs primarily focus on manipulating spatial waves, where the EM wave propagates in free space. However, MTSs also demonstrate the ability to manipulate surface waves, where the EM wave propagates along the tangential direction of the MTS.

In the optical frequency band, 2-D photonic crystals have been proposed as a means of manipulating surface light since the 1990s [165]–[168], and this remains a significant research area. To guide the surface wave with greater flexibility, photonic topological insulators [169]–[171] have also been artificially created, which can control the light propagation directions on the surface.

In the microwave band, periodic structures such as high-impedance surfaces (HISs) can manipulate surface

waves by forming electromagnetic band gaps (EBGs) that prohibit wave propagation along the MTS [172]–[175].

Furthermore, there have been studies on MTSs that facilitate the transition between surface waves and spatial waves. Phase-gradient metasurfaces can convert spatial EM waves to surface waves [176], while artificial impedance surfaces (AISs) can transform surface waves into directional spatial beams [177].

Despite significant advances in surface wave manipulation, research on R-MTSs for surface wave modulation is relatively limited compared to that of fixed surface-wave MTSs. A few reconfigurable MTSs have been proposed for dynamic surface wave manipulation. Early works introduced tunable EBG structures based on varactors [178], and more recently, a reprogrammable topological insulator operating in the microwave band was proposed [179]. As illustrated in Figure 10, the configuration of elements in the proposed system can be adjusted using two states of PIN diodes, enabling dynamic modulation of the propagation direction of surface waves.
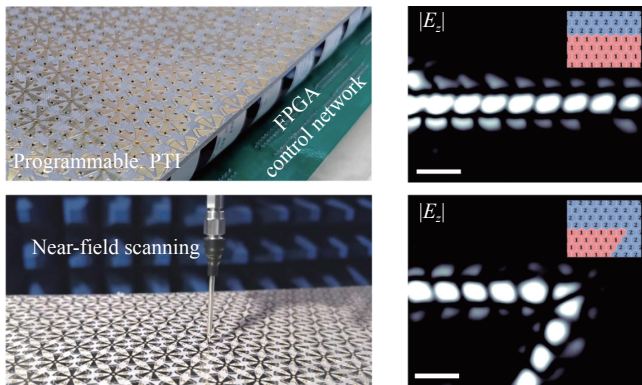
Figure 10 Reprogrammable topological insulator in the microwave band [179]. The propagation directions on the surface are programmed by independently addressing the configurations of the elements.

The high degree of flexibility offered by reconfigurable MTSs in manipulating surface waves highlights the high potential for future investigations in this area.
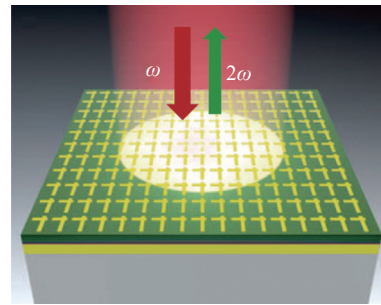
4. Nonlinear R-MTSs

Linear MTSs have been extensively researched, but to achieve greater functionality, nonlinear effects need to be considered in the design of MTS. Strictly speaking, reconfiguration is a form of nonlinearity that occurs at the state-transition moment. However, when an R-MTS is in a stable working state, its response to incident EM waves remains linear. Therefore, the R-MTS is essentially quasilinear.

Nonlinear MTSs, on the other hand, exhibit a consistently nonlinear response. Some forms of nonlinear effects include energy amplification, new frequency generation, and certain magnet-free nonreciprocity effects. Based on these nonlinear effects, various nonlinear MTS designs have been developed over the years.

Energy amplification relies on the nonlinearity of materials. Early implementations of MTS amplifiers utilized

transistors [55]–[58], [93], while more recent designs have employed parametric amplification MTS elements based on varactors [59].

Frequency generation MTSs have been investigated since the 1980s [59], [78]. Quasioptical grid arrays with lumped nonlinear components have been introduced to enable spatial wave processing functions in the microwave band, such as oscillation [180], [181], frequency doubling [182] and frequency mixing [183]. In the optical frequency band, nonlinear materials have been used to create nonlinear MTSs [184]–[187], which exhibit second harmonic generation (SHG) or third harmonic generation (THG), as shown in Figure 11. In recent years, with the development of time-modulated MTSs, frequency reconfiguration using the time dimension has become a new research trend [80]–[69], [103]–[106].

Figure 11 Optical nonlinear MTS for second harmonic generation [184].

Magnet-free nonreciprocal MTSs have gained attention. To realize nonreciprocity without relying on magnetic effects, nonlinear effects are taken into consideration. By utilizing the nonreciprocity of amplifiers, nonreciprocal MTSs can amplify the forward wave while blocking the backward wave [129], [188], [189]. Additionally, time-modulated R-MTSs can modulate frequency and beam direction without reciprocity, further enabling nonreciprocal wave manipulation [190]–[192].

In addition to these applications, nonlinear MTSs can perform other functions, such as all-optical logic gates [193], energy-selective surfaces [194], and waveform-dependent absorbers [195]. These areas represent interesting topics for future research. Moreover, the combination of reconfigurable and nonlinear MTSs can provide dynamic functionalities and nonlinear effects, potentially leading to a broader research wave in the future.

VI. Conclusion

The R-MTS, as an advanced form of MTS, has been proposed to dynamically manipulate scattered waves. In recent years, numerous R-MTSs with different dimensions and functions have emerged. In this review, we begin by exploring the interactions among R-MTSs, EM waves and EM information in five dimensions and propose a mathematical model of R-MTSs in response to the five dimensions of incident EM waves. We then suggest a concept called the information allocation strategy, which provides a systematic

categorization of the different types of R-MTSs. Based on this strategy, 1-bit reconfigurable elements manipulating one of the five dimensions are first reviewed and categorized. Then, we proceed to review the advances in multidimensional and multifunctional 2-bit elements. The various 2-bit elements are divided into two large categories: 2-bit-manipulating types (15 kinds) and multiplexed-manipulating types (25 kinds). We provide a detailed review of the existing 2-bit elements within each category.

Given the rapid evolution of R-MTSs, diverse terminologies have arisen, making the overall research architecture confusing. Hopefully, R-MTSs that are reorganized and united under the presented information allocation strategy can provide a helpful perspective for researchers to identify development paths and future research trends. In this paper, we also highlight some types of multibit reconfigurable elements that have not yet been realized, such as some 2-bit-manipulating elements and many multiplexed-manipulating elements. In addition, we discuss some potential evolution directions of R-MTSs, including multibit R-MTSs, THz/optical R-MTSs, surface-wave R-MTSs, nonlinear R-MTSs, and others.

As a recent highlight in both science and engineering fields, the exploration of R-MTSs is still unfolding. The R-MTS presents significant opportunities for critical applications in communication, detection, sensing, imaging and computing. For example, reconfigurable intelligent surfaces (RISs), possessing the remarkable ability to dynamically manipulate wireless channels and enhance wireless signals, have emerged as promising candidates for the forthcoming generation of wireless communications [196]–[199]. In addition, R-MTSs serve as programmable diffractive deep neural networks [200], which can propel optical computing technology. In summary, it is widely believed that R-MTSs will lead to a technological revolution in the near future.

Acknowledgements

References

[1] P. Nayeri, F. Yang, and A. Z. Elsherbeni, *Reflectarray Antennas: Theory, Designs, and Applications*, John Wiley & Sons, Hoboken, NJ, USA, 2018.

[2] N. I. Landy, S. Sajuyigbe, J. J. Mock, *et al*., "Perfect metamaterial absorber," *Physical Review Letters*, vol. 100, no. 20, article no. 207402, 2008.

[3] X. J. Ni, Z. J. Wong, M. Mrejen, *et al*., "An ultrathin invisibility skin cloak for visible light," *Science*, vol. 349, no. 6254, pp. 1310–1314, 2015.

[4] X. J. Ni, A. V. Kildishev, and V. M. Shalaev, "Metasurface holograms for visible light," *Nature Communications*, vol. 4, no. 1, article no. 2807, 2013.

[5] G. X. Zheng, H. Mühlenbernd, M. Kenney, *et al*. *Nanotechnology*, vol. 10, no. 4, pp. 308–312, 2015.

[6] M. Khorasaninejad, W. T. Chen, R. C. Devlin, *et al*., "Metalenses at visible wavelengths: Diffraction-limited focusing and subwavelength resolution imaging," *Science*, vol. 352, no. 6290, pp. 1190–1194, 2016.

[7] Q. He, S. L. Sun, and L. Zhou, "Tunable/reconfigurable metasurfaces: Physics and applications," *Research*, vol. 2019, article no. 1849272, 2019.

[8] Y. J. Feng, Q. Hu, K. Qu, *et al*., "Reconfigurable intelligent surfaces: Design, implementation, and practical demonstration," *Electromagnetic Science*, vol. 1, no. 2, article no. 0020111, 2023.

[9] Y. Saifullah, Y. J. He, A. Boag, *et al*., "Recent progress in reconfigurable and intelligent metasurfaces: A comprehensive review of tuning mechanisms, hardware designs, and applications," *Advanced Science*, vol. 9, no. 33, article no. 2203747, 2022.

[10] O. A. M. Abdelraouf, Z. Y. Wang, H. L. Liu, *et al*., "Recent advances in tunable metasurfaces: Materials, design, and applications," *ACS Nano*, vol. 16, no. 9, pp. 13339–13369, 2022.

[11] S. L. Sun, Q. He, J. M. Hao, *et al*., "Electromagnetic metasurfaces: Physics and applications," *Advances in Optics and Photonics*, vol. 11, no. 2, pp. 380–479, 2019.

[12] T. Gu, H. J. Kim, C. Rivero-Baleine, *et al*., "Reconfigurable metasurfaces towards commercial success," *Nature Photonics*, vol. 17, no. 1, pp. 48–58, 2023.

[13] T. J. Cui, M. Q. Qi, X. Wan, *et al*., "Coding metamaterials, digital metamaterials and programmable metamaterials," *Light: Science & Applications*, vol. 3, no. 10, article no. e218, 2014.

[14] F. Yang and Y. Rahmat-Samii, *Surface Electromagnetics: With Applications in Antenna, Microwave, and Optical Engineering*. Cambridge University Press, Cambridge, UK, 2019.

[15] T. J. Cui, S. Liu, and L. Zhang, "Information metamaterials and metasurfaces," *Journal of Materials Chemistry C*, vol. 5, no. 15, pp. 3644–3668, 2017.

[16] H. H. Yang, X. Y. Cao, F. Yang, *et al*., "A programmable metasurface with dynamic polarization, scattering and focusing control," *Scientific Reports*, vol. 6, no. 1, article no. 35692, 2016.

[17] X. T. Pan, F. Yang, S. H. Xu, *et al*., "A 10 240-element reconfigurable reflectarray with fast steerable monopulse patterns," *IEEE Transactions on Antennas and Propagation*, vol. 69, no. 1, pp. 173–181, 2021.

[18] T. Shan, X. T. Pan, M. K. Li, *et al*, "Coding programmable metasurfaces based on deep learning techniques," *IEEE Journal on Emerging and Selected Topics in Circuits and Systems*, vol. 10, no. 1, pp. 114–125, 2020.

[19] Z. Y. Wang, X. T. Pan, F. Yang, *et al*., "Design, analysis, and experiment on high-performance orbital angular momentum beam based on 1-bit programmable metasurface," *IEEE Access*, vol. 9, pp. 18585–18596, 2021.

[20] S. V. Hum and J. Perruisseau-Carrier, "Reconfigurable reflectarrays and array lenses for dynamic antenna beam control: A review," *IEEE Transactions on Antennas and Propagation*, vol. 62, no. 1, pp. 183–198, 2014.

[21] X. Yang, S. H. Xu, F. Yang, *et al*., "A broadband high-efficiency reconfigurable reflectarray antenna using mechanically rotational elements," *IEEE Transactions on Antennas and Propagation*, vol. 65, no. 8, pp. 3959–3966, 2017.

[22] Y. L. Zheng, K. Chen, W. X. Yang, *et al*., "Kirigami reconfigurable gradient metasurface," *Advanced Functional Materials*, vol. 32, no. 5, article no. 2107699, 2022.

[23] A. Komar, R. Paniagua-Domínguez, A. Miroshnichenko, *et al*., "Dynamic beam switching by liquid crystal tunable dielectric metasurfaces," *ACS Photonics*, vol. 5, no. 5, pp. 1742–1748, 2018.

[24] X. G. Zhang, W. X. Jiang, H. L. Jiang, *et al*., "An optically driven digital metasurface for programming electromagnetic functions," *Nature Electronics*, vol. 3, no. 3, pp. 165–171, 2020.

[25] S. Y. Miao and F. H. Lin, "Light-controlled large-scale wirelessly reconfigurable microstrip reflectarrays," *IEEE Transactions on Antennas and Propagation*, vol. 71, no. 2, pp. 1613–1622, 2023.

[26] I. Zubritskaya, N. Maccaferri, X. I. Ezeiza, *et al*., "Magnetic con-

trol of the chiroptical plasmonic sur faces," *Nano Letters*, vol. 18, no. 1, pp. 302–307, 2018.

[27] L. L. Li, T. J. Cui, W. Ji, *et al*., "Electromagnetic reprogrammable coding-metasurface holograms," *Nature Communications*, vol. 8, no. 1, article no. 197, 2017.

[28] H. H. Yang, F. Yang, S. H. Xu, *et al*., "A study of phase quantization effects for reconfigurable reflectarray antennas," *IEEE Antennas and Wireless Propagation Letters*, vol. 16, pp. 302–305, 2016.

[29] B. Wu, A. Sutinjo, M. E. Potter, *et al*., "On the selection of the number of bits to control a dynamic digital MEMS reflectarray," *IEEE Antennas and Wireless Propagation Letters*, vol. 7, pp. 183–186, 2008.

[30] P. Nayeri, F. Yang, and A. Z. Elsherbeni, "Beam-scanning reflectarray antennas: A technical overview and state of the art," *IEEE Antennas and Propagation Magazine*, vol. 57, no. 4, pp. 32–47, 2015.

[31] H. H. Yang, F. Yang, S. H. Xu, *et al*., "A 1-bit 10 × 10 reconfigurable reflectarray antenna: Design, optimization, and experiment," *IEEE Transactions on Antennas and Propagation*, vol. 64, no. 6, pp. 2246–2254, 2016.

[32] H. H. Yang, F. Yang, X. Y. Cao, *et al*., "A 1600-element dual-frequency electronically reconfigurable reflectarray at X/Ku-band," *IEEE Transactions on Antennas and Propagation*, vol. 65, no. 6, pp. 3024–3032, 2017.

[33] H. Kamoda, T. Iwasaki, J. Tsumochi, *et al*., "60-GHz electronically reconfigurable large reflectarray using single-bit phase shifters," *IEEE Transactions on Antennas and Propagation*, vol. 59, no. 7, pp. 2524–2531, 2011.

[34] X. T. Pan, S. D. Wang, G. F. Li, *et al*., "On-chip reconfigurable reflectarray for 2-d beam-steering at w-band," in *2018 IEEE MTT-S International Wireless Symposium (IWS)*, Chengdu, China, pp. 1–4, 2018.

[35] B. J. Xiang, X. Dai, and K. M. Luk, "A wideband low-cost reconfigurable reflectarray antenna with 1-bit resolution," *IEEE Transactions on Antennas and Propagation*, vol. 70, no. 9, pp. 7439–7447, 2022.

[36] F. Wu, R. Lu, J. X. Wang, *et al*., "A circularly polarized 1 bit electronically reconfigurable reflectarray based on electromagnetic element rotation," *IEEE Transactions on Antennas and Propagation*, vol. 69, no. 9, pp. 5585–5595, 2021.

[37] M. Cerveny, K. L. Ford, and A. Tennant, "Reflective switchable polarization rotator based on metasurface with pin diodes," *IEEE Transactions on Antennas and Propagation*, vol. 69, no. 3, pp. 1483–1492, 2021.

[38] Z. L. Wang, Y. H. Ge, J. X. Pu, *et al*., "1 bit electronically reconfigurable folded reflectarray antenna based on p-i-n diodes for wide-angle beam-scanning applications," *IEEE Transactions on Antennas and Propagation*, vol. 68, no. 9, pp. 6806–6810, 2020.

[39] M. T. Zhang, S. Gao, Y. C. Jiao, *et al*., "Design of novel reconfigurable reflectarrays with single-bit phase resolution for ku-band satellite antenna applications," *IEEE Transactions on Antennas and Propagation*, vol. 64, no. 5, pp. 1634–1641, 2016.

[40] F. Wu, R. Lu, J. X. Wang, *et al*., "Circularly polarized one-bit reconfigurable me-dipole reflectarray at x-band," *IEEE Antennas and Wireless Propagation Letters*, vol. 21, no. 3, pp. 496–500, 2021.

[41] H. H. Yang, F. Yang, S. H. Xu, *et al*., "A 1-bit multipolarization reflectarray element for reconfigurable large-aperture antennas," *IEEE Antennas and Wireless Propagation Letters*, vol. 16, pp. 581–584, 2016.

[42] C. H. Liu, Y. Wu, F. Yang, *et al*., "Is it possible to design a 1-bit reconfigurable transmitarray element with a single switch?," *IEEE Antennas and Wireless Propagation Letters*, vol. 22, no. 4, pp. 829–833, 2023.

[43] A. Clemente, L. Dussopt, R. Sauleau, *et al*., "1-bit reconfigurable unit cell based on PIN diodes for transmit-array applications in *x*-band," *IEEE Transactions on Antennas and Propagation*, vol. 60, no. 5, pp. 2260–2269, 2012.

[44] A. Clemente, L. Dussopt, R. Sauleau, *et al*., "Wideband 400-element electronically reconfigurable transmitarray in X band," *IEEE Transactions on Antennas and Propagation*, vol. 61, no. 10, pp. 5017–5027, 2013.

[45] M. Wang, S. H. Xu, N. Hu, *et al*., "Design and measurement of a *Ku*-band pattern-reconfigurable array antenna using 16 O-slot patch elements with p-i-n diodes," *IEEE Antennas and Wireless Propagation Letters*, vol. 19, no. 12, pp. 2373–2377, 2020.

[46] Y. Wang, S. H. Xu, F. Yang, *et al*., "A novel 1 bit wide-angle beam scanning reconfigurable transmitarray antenna using an equivalent magnetic dipole element," *IEEE Transactions on Antennas and Propagation*, vol. 68, no. 7, pp. 5691–5695, 2020.

[47] M. Wang, S. H. Xu, F. Yang, *et al*., "Design of a ku-band 1-bit reconfigurable transmitarray with 16×16 slot coupled elements," in *2017 IEEE International Symposium on Antennas and Propagation & USNC/URSI National Radio Science Meeting*, San Diego, CA, USA, pp. 1991–1992, 2017.

[48] C. W. Luo, G. Zhao, Y. C. Jiao, *et al*., "Wideband 1 bit reconfigurable transmitarray antenna based on polarization rotation element," *IEEE Antennas and Wireless Propagation Letters*, vol. 20, no. 5, pp. 798–802, 2021.

[49] H. Yu, J. X. Su, Z. R. Li, *et al*., "A novel wideband and high-efficiency electronically scanning transmitarray using transmission metasurface polarizer," *IEEE Transactions on Antennas and Propagation*, vol. 70, no. 4, pp. 3088–3093, 2022.

[50] B. D. Nguyen and C. Pichot, "Unit-cell loaded with PIN diodes for 1-bit linearly polarized reconfigurable transmitarrays," *IEEE Antennas and Wireless Propagation Letters*, vol. 18, no. 1, pp. 98–102, 2019.

[51] X. Wang, P. Y. Qin, A. T. Le, *et al*., "Beam scanning transmitarray employing reconfigurable dual-layer Huygens element," *IEEE Transactions on Antennas and Propagation*, vol. 70, no. 9, pp. 7491–7500, 2022.

[52] M. Wang, S. H. Xu, F. Yang, *et al*., "A 1-bit bidirectional reconfigurable transmit-reflect-array using a single-layer slot element with pin diodes," *IEEE Transactions on Antennas and Propagation*, vol. 67, no. 9, pp. 6205–6210, 2019.

[53] Q. R. Hong, Q. Ma, X. X. Gao, *et al*., "Programmable amplitude-coding metasurface with multifrequency modulations," *Advanced Intelligent Systems*, vol. 3, no. 8, article no. 2000260, 2021.

[54] Z. J. Zhang, L. L. Dai, X. B. Chen, *et al*., "Active RIS vs. passive RIS: Which will prevail in 6G?," *IEEE Transactions on Communications*, vol. 71, no. 3, pp. 1707–1725, 2023.

[55] J. Lin and T. Itoh, "Active integrated antennas," *IEEE Transactions on Microwave Theory and Techniques*, vol. 42, no. 12, pp. 2186–2194, 1994.

[56] M. Kim, E. A. Sovero, J. B. Hacker, *et al*., "A 100-element HBT grid amplifier," *IEEE Transactions on Microwave Theory and Techniques*, vol. 41, no. 10, pp. 1762–1771, 1993.

[57] M. Kim, J. J. Rosenberg, R. P. Smith, *et al*., "A grid amplifier," *IEEE Microwave and Guided Wave Letters*, vol. 1, no. 11, pp. 322–324, 1991.

[58] M. E. Bialkowski, A. W. Robinson, and H. J. Song, "Design, development, and testing of X-band amplifying reflectarrays," *IEEE Transactions on Antennas and Propagation*, vol. 50, no. 8, pp. 1065–1076, 2002.

[59] X. Chen and F. Yang, "Nonlinear electromagnetic surfaces: Theory, design and application," *Master thesis*, Tsinghua University, Beijing, China, 2020.

[60] H. Jeong, D. H. Le, D. Lim, *et al*., "Reconfigurable metasurfaces for frequency selective absorption," *Advanced Optical Materials*, vol. 8, no. 13, article no. 1902182, 2020.

[61] B. Zhu, C. Huang, Y. J. Feng, *et al*., "Dual band switchable metamaterial electromagnetic absorber," *Progress in Electromagnetics Research B*, vol. 24, pp. 121–129, 2010.

[62] Y. Li, J. Lin, H. J. Guo, *et al*., "A tunable metasurface with switchable functionalities: From perfect transparency to perfect absorption," *Advanced Optical Materials*, vol. 8, no. 6, article no.

1901548, 2020.

[63] B. Zhu, Y. J. Feng, J. M. Zhao, *et al*., "Switchable metamaterial reflector/absorber for different polarized electromagnetic waves," *Applied Physics Letters*, vol. 97, no. 5, article no. 051906, 2010.

[64] S. Ghosh and K. V. Srivastava, "Polarization-insensitive single- and broadband switchable absorber/reflector and its realization using a novel biasing technique," *IEEE Transactions on Antennas and Propagation*, vol. 64, no. 8, pp. 3665–3670, 2016.

[65] H. C. Yu, X. Y. Cao, J. Gao, *et al*., "Design of a wideband and reconfigurable polarization converter using a manipulable metasurface," *Optical Materials Express*, vol. 8, no. 11, pp. 3373–3381, 2018.

[66] X. L. Ma, W. B. Pan, C. Huang, *et al*., "An active metamaterial for polarization manipulating," *Advanced Optical Materials*, vol. 2, no. 10, pp. 945–949, 2014.

[67] A. Edalati and T. A. Denidni, "Frequency selective surfaces for beam-switching applications," *IEEE Transactions on Antennas and Propagation*, vol. 61, no. 1, pp. 195–200, 2013.

[68] W. J. Liao, Y. F. Chen, C. L. Liao, *et al*., "Reconfigurable frequency selective surfaces with complementary reflection and transmission responses using duality theorem-based elements," *IEEE Transactions on Antennas and Propagation*, vol. 70, no. 10, pp. 9406–9414, 2022.

[69] S. Taravati and G. V. Eleftheriades, "Pure and linear frequency-conversion temporal metasurface," *Physical Review Applied*, vol. 15, no. 6, article no. 064011, 2021.

[70] P. M. Sainadh, A. Sharma, and S. Ghosh, "Polarization-insensitive absorptive/transmissive reconfigurable frequency selective surface with embedded biasing," *IEEE Antennas and Wireless Propagation Letters*, vol. 22, no. 1, pp. 164–168, 2022.

[71] C. X. Huang, J. J. Zhang, Q. Cheng, *et al*., "Polarization modulation for wireless communications based on metasurfaces," *Advanced Functional Materials*, vol. 31, no. 36, article no. 2103379, 2021.

[72] F. Ding, S. W. Tang, and S. I. Bozhevolnyi, "Recent advances in polarization-encoded optical metasurfaces," *Advanced Photonics Research*, vol. 2, no. 6, article no. 2000173, 2021.

[73] Y. Q. Hu, X. D. Wang, X. H. Luo, *et al*., "All-dielectric metasurfaces for polarization manipulation: Principles and emerging applications," *Nanophotonics*, vol. 9, no. 12, pp. 3755–3780, 2020.

[74] T. T. Lv, Y. X. Li, H. F. Ma, *et al*., "Hybrid metamaterial switching for manipulating chirality based on VO₂ phase transition," *Scientific Reports*, vol. 6, no. 1, article no. 23186, 2016.

[75] K. Chen, Y. J. Feng, L. Cui, *et al*., "Dynamic control of asymmetric electromagnetic wave transmission by active chiral metamaterial," *Scientific Reports*, vol. 7, no. 1, article no. 42802, 2017.

[76] B. Liang, B. Sanz-Izquierdo, E. A. Parker, *et al*., "Cylindrical slot FSS configuration for beam-switching applications," *IEEE Transactions on Antennas and Propagation*, vol. 63, no. 1, pp. 166–173, 2015.

[77] R. Y. Wu, L. Zhang, L. Bao, *et al*., "Digital metasurface with phase code and reflection-transmission amplitude code for flexible full-space electromagnetic manipulations," *Advanced Optical Materials*, vol. 7, no. 8, article no. 1801429, 2019.

[78] M. P. DeLisio and R. A. York, "Quasi-optical and spatial power combining," *IEEE Transactions on Microwave Theory and Techniques*, vol. 50, no. 3, pp. 929–936, 2002.

[79] P. Rocca, Q. J. Zhu, E. T. Bekele, *et al*., "4-D arrays as enabling technology for cognitive radio systems," *IEEE Transactions on Antennas and Propagation*, vol. 62, no. 3, pp. 1102–1116, 2014.

[80] A. Shaltout, A. Kildishev, and V. Shalaev, "Time-varying metasurfaces and Lorentz non-reciprocity," *Optical Materials Express*, vol. 5, no. 11, pp. 2459–2467, 2015.

[81] Z. Z. Liu, Z. Y. Li, and K. Aydin, "Time-varying metasurfaces based on graphene microribbon arrays," *ACS Photonics*, vol. 3, no. 11, pp. 2035–2039, 2016.

[82] Y. Hadad, D. L. Sounas, and A. Alu, "Space-time gradient metasurfaces," *Physical Review B*, vol. 92, no. 10, article no. 100304, 2015.

[83] C. Huang, B. Sun, W. B. Pan, *et al*., "Dynamical beam manipulation based on 2-bit digitally-controlled coding metasurface," *Scientific Reports*, vol. 7, no. 1, article no. 42302, 2017.

[84] B. D. Nguyen, V. S. Tran, L. Mai, *et al*., "A two-bit reflectarray element using cut-ring patch coupled to delay lines," *REV Journal on Electronics and Communications*, vol. 6, pp. 1–2, 2016.

[85] F. Diaby, A. Clemente, R. Sauleau, *et al*., "2 bit reconfigurable unit-cell and electronically steerable transmitarray at *Ka*-band," *IEEE Transactions on Antennas and Propagation*, vol. 68, no. 6, pp. 5003–5008, 2020.

[86] C. C. Cheng and A. Abbaspour-Tamijani, "Design and experimental verification of steerable reflect-arrays based on two-bit antenna-filter-antenna elements," in *2009 IEEE MTT-S International Microwave Symposium Digest*, Boston, MA, USA, pp. 1181–1184, 2009.

[87] Q. S. Zhang, M. T. Zhang, X. W. Shi, *et al*., "A low-profile beam-steering reflectarray with integrated leaky-wave feed and 2-Bit phase resolution for Ka-band SatCom," *IEEE Transactions on Antennas and Propagation*, vol. 70, no. 3, pp. 1884–1894, 2022.

[88] X. Yang, S. H. Xu, F. Yang, *et al*., "A novel 2-bit reconfigurable reflectarray element for both linear and circular polarizations," in *2017 IEEE International Symposium on Antennas and Propagation & USNC/URSI National Radio Science Meeting*, San Diego, CA, USA, pp. 2083–2084, 2017.

[89] L. Chen, Q. Ma, H. B. Jing, *et al*., "Space-energy digital-coding metasurface based on an active amplifier," *Physical Review Applied*, vol. 11, no. 5, article no. 054051, 2019.

[90] J. H. Cui, C. Huang, W. B. Pan, *et al*., "Dynamical manipulation of electromagnetic polarization using anisotropic meta-mirror," *Scientific Reports*, vol. 6, no. 1, article no. 30771, 2016.

[91] C. Huang, J. M. Liao, C. Ji, *et al*., "Graphene-integrated reconfigurable metasurface for independent manipulation of reflection magnitude and phase," *Advanced Optical Materials*, vol. 9, no. 7, article no. 2001950, 2021.

[92] J. M. Liao, S. J. Guo, L. M. Yuan, *et al*., "Independent manipulation of reflection amplitude and phase by a single-layer reconfigurable metasurface," *Advanced Optical Materials*, vol. 10, no. 4, article no. 2101551, 2022.

[93] K. K. Kishor and S. V. Hum, "An amplifying reconfigurable reflectarray antenna," *IEEE Transactions on Antennas and Propagation*, vol. 60, no. 1, pp. 197–205, 2012.

[94] J. Perruisseau-Carrier, "Dual-polarized and polarization-flexible reflective cells with dynamic phase control," *IEEE Transactions on Antennas and Propagation*, vol. 58, no. 5, pp. 1494–1502, 2010.

[95] T. Debogović, S. Sušsac, and J. Perruisseau-Carrier, "A simple reflectarray cell with 1-bit phase control and polarization flexibility," in *2013 7th European Conference on Antennas and Propagation (EuCAP)*, Gothenburg, Sweden, pp. 2717–2720, 2013.

[96] W. B. Pan, C. Huang, X. L. Ma, *et al*., "A dual linearly polarized transmitarray element with 1-bit phase resolution in x-band," *IEEE Antennas and Wireless Propagation Letters*, vol. 14, pp. 167–170, 2014.

[97] C. Huang, W. B. Pan, X. L. Ma, *et al*., "1-bit reconfigurable circularly polarized transmitarray in X-band," *IEEE Antennas and Wireless Propagation Letters*, vol. 15, pp. 448–451, 2015.

[98] G. Y. Liu, H. X. Liu, J. Q. Han, *et al*., "Reconfigurable metasurface with polarization-independent manipulation for reflection and transmission wavefronts," *Journal of Physics D: Applied Physics*, vol. 53, no. 4, article no. 045107, 2019.

[99] Q. Hu, J. M. Zhao, K. Chen, *et al*., "An intelligent programmable Omni-metasurface," *Laser & Photonics Reviews*, vol. 16, no. 6, article no. 2100718, 2022.

[100] H. Yu, P. Li, J. X. Su, *et al*., "Reconfigurable bidirectional beam-steering aperture with transmitarray, reflectarray, and transmit-reflect-array modes switching," *IEEE Transactions on Antennas and Propagation*, vol. 71, no. 1, pp. 581–595, 2023.

[101] R. Phon, S. Ghosh, and S. Lim, "Novel multifunctional reconfigurable active frequency selective surface," *IEEE Transactions on Antennas and Propagation*, vol. 67, no. 3, pp. 1709–1718, 2019.

[102] L. Chen, Q. Ma, Q. F. Nie, *et al*., "Dual-polarization programmable metasurface modulator for near-field information encoding and transmission," *Photonics Research*, vol. 9, no. 2, pp. 116–124, 2021.

[103] L. Zhang, X. Q. Chen, S. Liu, *et al*., "Space-time-coding digital metasurfaces," *Nature Communications*, vol. 9, no. 1, article no. 4334, 2018.

[104] X. Wang, J. Q. Han, S. C. Tian, *et al*., "Amplification and manipulation of nonlinear electromagnetic waves and enhanced nonreciprocity using transmissive space-time-coding metasurface," *Advanced Science*, vol. 9, no. 11, article no. 2105960, 2022.

[105] Q. Hu, K. Chen, J. M. Zhao, *et al*., "On-demand dynamic polarization meta-transformer," *Laser & Photonics Reviews*, vol. 17, no. 1, article no. 2200479, 2023.

[106] M. K. Liu, D. A. Powell, Y. Zarate, *et al*., "Huygens' metadevices for parametric waves," *Physical Review X*, vol. 8, no. 3, article no. 031077, 2018.

[107] X. Y. Song, W. X. Yang, K. Qu, *et al*., "Switchable metasurface for nearly perfect reflection, transmission, and absorption using pin diodes," *Optics Express*, vol. 29, no. 18, pp. 29320–29328, 2021.

[108] J. Y. Dai, J. Zhao, Q. Cheng, *et al*., "Independent control of harmonic amplitudes and phases via a time-domain digital coding metasurface," *Light: Science & Applications*, vol. 7, no. 1, article no. 90, 2018.

[109] J. Zhao, X. Yang, J. Y. Dai, *et al*., "Programmable time-domain digital-coding metasurface for non-linear harmonic manipulation and new wireless communication systems," *National Science Review*, vol. 6, no. 2, pp. 231–238, 2019.

[110] L. Zhang, M. Z. Chen, W. K. Tang, *et al*., "A wireless communication scheme based on space- and frequency-division multiplexing using digital metasurfaces," *Nature Electronics*, vol. 4, no. 3, pp. 218–227, 2021.

[111] M. Z. Chen, W. K. Tang, J. Y. Dai, *et al*., "Accurate and broadband manipulations of harmonic amplitudes and phases to reach 256 QAM millimeter-wave wireless communications by time-domain digital coding metasurface," *National Science Review*, vol. 9, no. 1, article no. nwab134, 2022.

[112] Q. Hu, K. Chen, N. Zhang, *et al*., "Arbitrary and dynamic poincaré sphere polarization converter with a time-varying metasurface," *Advanced Optical Materials*, vol. 10, no. 4, article no. 2101915, 2022.

[113] C. Guclu, J. Perruisseau-Carrier, and O. Civi, "Proof of concept of a dual-band circularly-polarized RF MEMS beam-switching reflectarray," *IEEE Transactions on Antennas and Propagation*, vol. 60, no. 11, pp. 5451–5455, 2012.

[114] E. Baladi, M. Y. Xu, N. Faria, *et al*., "Dual-band circularly polarized fully reconfigurable reflectarray antenna for satellite applications in the Ku-band," *IEEE Transactions on Antennas and Propagation*, vol. 69, no. 12, pp. 8387–8396, 2021.

[115] N. Zhang, K. Chen, Y. L. Zheng, *et al*., "Programmable coding metasurface for dual-band independent real-time beam control," *IEEE Journal on Emerging and Selected Topics in Circuits and Systems*, vol. 10, no. 1, pp. 20–28, 2020.

[116] T. Debogovic and J. Perruisseau-Carrier, "Low loss MEMS-reconfigurable 1-bit reflectarray cell with dual-linear polarization," *IEEE Transactions on Antennas and Propagation*, vol. 62, no. 10, pp. 5055–5060, 2014.

[117] X. G. Zhang, Q. Yu, W. X. Jiang, *et al*., "Polarization-controlled dual-programmable metasurfaces," *Advanced Science*, vol. 7, no. 11, article no. 1903382, 2020.

[118] L. B. Yan, W. M. Zhu, M. F. Karim, *et al*., "Arbitrary and independent polarization control in situ via a single metasurface," *Advanced Optical Materials*, vol. 6, no. 21, article no. 1800728, 2018.

[119] H. J. Xu, S. H. Xu, F. Yang, *et al*., "Design and experiment of a dual-band 1 bit reconfigurable reflectarray antenna with independent large-angle beam scanning capability," *IEEE Antennas and Wireless Propagation Letters*, vol. 19, no. 11, pp. 1896–1900, 2020.

[120] Y. Wang, S. H. Xu, F. Yang, *et al*., "1 bit dual-linear polarized reconfigurable transmitarray antenna using asymmetric dipole elements with parasitic bypass dipoles," *IEEE Transactions on Antennas and Propagation*, vol. 69, no. 2, pp. 1188–1192, 2021.

[121] X. L. Zhang, F. Yang, S. H. Xu, *et al*., "Single-layer reflectarray antenna with independent dual-CP beam control," *IEEE Antennas and Wireless Propagation Letters*, vol. 19, no. 4, pp. 532–536, 2020.

[122] J. P. B. Mueller, N. A. Rubin, R. C. Devlin, *et al*., "Metasurface polarization optics: Independent phase control of arbitrary orthogonal states of polarization," *Physical Review Letters*, vol. 118, no. 11, article no. 113901, 2017.

[123] C. S. Geaney, M. Hosseini, and S. V. Hum, "Reflectarray antennas for independent dual linear and circular polarization control," *IEEE Transactions on Antennas and Propagation*, vol. 67, no. 9, pp. 5908–5918, 2019.

[124] S. Mener, R. Gillard, R. Sauleau, *et al*., "Dual circularly polarized reflectarray with independent control of polarizations," *IEEE Transactions on Antennas and Propagation*, vol. 63, no. 4, pp. 1877–1881, 2015.

[125] H. Y. Li, Q. S. Cao, and Y. Wang, "A novel 2-B multifunctional active frequency selective surface for LTE-2.1 GHz," *IEEE Transactions on Antennas and Propagation*, vol. 65, no. 6, pp. 3084–3092, 2017.

[126] H. Y. Li, Q. S. Cao, L. L. Liu, *et al*., "An improved multifunctional active frequency selective surface," *IEEE Transactions on Antennas and Propagation*, vol. 66, no. 4, pp. 1854–1862, 2018.

[127] Y. Li, Y. Wang, and Q. S. Cao, "Design of a multifunctional reconfigurable metasurface for polarization and propagation manipulation," *IEEE Access*, vol. 7, pp. 129183–129191, 2019.

[128] L. W. Wu, H. F. Ma, R. Y. Wu, *et al*., "Transmission reflection controls and polarization controls of electromagnetic holograms by a reconfigurable anisotropic digital coding metasurface," *Advanced Optical Materials*, vol. 8, no. 22, article no. 2001065, 2020.

[129] Q. Ma, L. Chen, H. B. Jing, *et al*., "Controllable and programmable nonreciprocity based on detachable digital coding metasurface," *Advanced Optical Materials*, vol. 7, no. 24, article no. 1901285, 2019.

[130] K. Chen, G. W. Ding, G. W. Hu, *et al*., "Directional janus metasurface," *Advanced Materials*, vol. 32, no. 2, article no. 1906352, 2020.

[131] P. Yu, J. X. Li, S. Zhang, *et al*., "Dynamic janus metasurfaces in the visible spectral region," *Nano letters*, vol. 18, no. 7, pp. 4584–4589, 2018.

[132] S. M. Kamali, E. Arbabi, A. Arbabi, *et al*., "Angle-multiplexed metasurfaces: Encoding independent wavefronts in a single metasurface under different illumination angles," *Physical Review X*, vol. 7, no. 4, article no. 041056, 2017.

[133] Y. J. Bao, Y. Yu, H. F. Xu, *et al*., "Coherent pixel design of metasurfaces for multidimensional optical control of multiple printing-image switching and encoding," *Advanced Functional Materials*, vol. 28, no. 51, article no. 1805306, 2018.

[134] E. L. Wang, J. B. Niu, Y. H. Liang, *et al*., "Complete control of multichannel, angle-multiplexed, and arbitrary spatially varying polarization fields," *Advanced Optical Materials*, vol. 8, no. 6, article no. 1901674, 2020.

[135] J. Jang, G. Y. Lee, J. Sung, *et al*., "Independent multichannel wavefront modulation for angle multiplexed meta-holograms," *Advanced Optical Materials*, vol. 9, no. 17, article no. 2100678, 2021.

[136] S. Wan, C. W. Wan, C. J. Dai, *et al*., "Angular-multiplexing metasurface: Building up independent-encoded amplitude/phase dictio-

nary for angular illumination," *Advanced Optical Materials*, vol. 9, no. 22, article no. 2101547, 2021.

[137] X. Y. Zhang, Q. Li, F. F. Liu, *et al*., "Controlling angular dispersions in optical metasurfaces," *Light: Science & Applications*, vol. 9, no. 1, article no. 76, 2020.

[138] R. Pereira, R. Gillard, R. Sauleau, *et al*., "Dual linearly-polarized unit-cells with nearly 2-bit resolution for reflectarray applications in X-band," *IEEE Transactions on Antennas and Propagation*, vol. 60, no. 12, pp. 6042–6048, 2012.

[139] S. Venkatesh, X. Y. Lu, H. Saeidi, *et al*., "A high-speed programmable and scalable terahertz holographic metasurface based on tiled CMOS chips," *Nature Electronics*, vol. 3, no. 12, pp. 785–793, 2020.

[140] H. T. Chen, W. J. Padilla, J. M. O. Zide, *et al*., "Active terahertz metamaterial devices," *Nature*, vol. 444, no. 7119, pp. 597–600, 2006.

[141] H. T. Chen, W. J. Padilla, M. J. Cich, *et al*., "A metamaterial solid-state terahertz phase modulator," *Nature Photonics*, vol. 3, no. 3, pp. 148–151, 2009.

[142] H. J. Xu, S. H. Xu, F. Yang, *et al*., "Design of a terahertz reconfigurable reflectarray with individually controlled 1-bit phasing elements," in *2019 IEEE International Symposium on Antennas and Propagation and USNC-URSI Radio Science Meeting*, Atlanta, GA, USA, pp. 309–310, 2019.

[143] Y. X. Zhang, Y. C. Zhao, S. X. Liang, *et al*., "Large phase modulation of THz wave via an enhanced resonant active HEMT metasurface," *Nanophotonics*, vol. 8, no. 1, pp. 153–170, 2018.

[144] Y. X. Zhang, S. Qiao, S. X. Liang, *et al*., "Gbps terahertz external modulator based on a composite metamaterial with a double-channel heterostructure," *Nano letters*, vol. 15, no. 5, pp. 3501–3506, 2015.

[145] Y. C. Zhao, L. Wang, Y. X. Zhang, *et al*., "High-speed efficient terahertz modulation based on tunable collective-individual state conversion within an active 3 nm two-dimensional electron gas metasurface," *Nano Letters*, vol. 19, no. 11, pp. 7588–7597, 2019.

[146] P. K. Singh and S. Sonkusale, "High speed terahertz modulator on the chip based on tunable terahertz slot waveguide," *Scientific Reports*, vol. 7, no. 1, article no. 40933, 2017.

[147] P. Q. Liu, I. J. Luxmoore, S. A. Mikhailov, *et al*., "Highly tunable hybrid metamaterials employing split-ring resonators strongly coupled to graphene surface plasmons," *Nature Communications*, vol. 6, article no. 8969, 2015.

[148] Z. F. Chen, X. Q. Chen, L. Tao, *et al*., "Graphene controlled Brewster angle device for ultra broadband terahertz modulation," *Nature Communications*, vol. 9, no. 1, article no. 4909, 2018.

[149] Y. S. Liu, T. Sun, Y. Xu, *et al*., "Active tunable THz metamaterial array implemented in CMOS technology," *Journal of Physics D: Applied Physics*, vol. 54, no. 8, article no. 085107, 2020.

[150] N. M. Monroe, G. C. Dogiamis, R. Stingel, *et al*., "Electronic THz pencil beam forming and 2d steering for high angular-resolution operation: A 98×98-unit 265ghz CMOS reflectarray with in-unit digital beam shaping and squint correction," in *2022 IEEE International Solid-State Circuits Conference (ISSCC)*, San Francisco, CA, USA, pp. 1–3, 2022.

[151] Y. C. Zhao, Y. X. Zhang, Q. W. Shi, *et al*., "Dynamic photoinduced controlling of the large phase shift of terahertz waves via vanadium dioxide coupling nanostructures," *ACS Photonics*, vol. 5, no. 8, pp. 3040–3050, 2018.

[152] B. W. Chen, J. B. Wu, W. L. Li, *et al*., "Programmable terahertz metamaterials with non-volatile memory," *Laser & Photonics Reviews*, vol. 16, no. 4, article no. 2100472, 2022.

[153] B. W. Chen, X. R. Wang, W. L. Li, *et al*., "Electrically addressable integrated intelligent terahertz metasurface," *Science Advances*, vol. 8, no. 41, article no. eadd1296, 2022.

[154] A. M. Shaltout, V. M. Shalaev, and M. L. Brongersma, "Spatiotemporal light control with active metasurfaces," *Science*, vol. 364, no. 6441, article no. eaat3100, 2019.

[155] Y. W. Huang, H. W. H. Lee, R. Sokhoyan, *et al*., "Gate-tunable conducting oxide metasurfaces," *Nano Letters*, vol. 16, no. 9, pp. 5319–5325, 2016.

[156] J. X. Li, P. Yu, H. Cheng, *et al*., "Optical polarization encoding using graphene-loaded plasmonic metasurfaces," *Advanced Optical Materials*, vol. 4, no. 1, pp. 91–98, 2016.

[157] Q. Wang, E. T. F. Rogers, B. Gholipour, *et al*., "Optically reconfigurable metasurfaces and photonic devices based on phase change materials," *Nature Photonics*, vol. 10, no. 1, pp. 60–65, 2016.

[158] A. Karvounis, B. Gholipour, K. F. MacDonald, *et al*., "All-dielectric phase-change reconfigurable metasurface," *Applied Physics Letters*, vol. 109, no. 5, article no. 051103, 2016.

[159] X. H. Yin, M. Schäferling, A. K. U. Michel, *et al*., "Active chiral plasmonics," *Nano Letters*, vol. 15, no. 7, pp. 4255–4260, 2015.

[160] Y. F. Wang, P. Landreman, D. Schoen, *et al*., "Electrical tuning of phase-change antennas and metasurfaces," *Nature Nanotechnology*, vol. 16, no. 6, pp. 667–672, 2021.

[161] Q. W. Lin, H. Wong, L. Huitema, *et al*., "Coding metasurfaces with reconfiguration capabilities based on optical activation of phase-change materials for terahertz beam manipulations," *Advanced Optical Materials*, vol. 10, no. 1, article no. 2101699, 2022.

[162] Y. F. Zhang, C. Fowler, J. H. Liang, *et al*., "Electrically reconfigurable non-volatile metasurface using low-loss optical phase-change material," *Nature Nanotechnology*, vol. 16, no. 6, pp. 661–666, 2021.

[163] S. Q. Li, X. W. Xu, R. M. Veetil, *et al*., "Phase-only transmissive spatial light modulator based on tunable dielectric metasurface," *Science*, vol. 364, no. 6445, pp. 1087–1090, 2019.

[164] J. Karst, M. Floess, M. Ubl, *et al*., "Electrically switchable metallic polymer nanoantennas," *Science*, vol. 374, no. 6567, pp. 612–616, 2021.

[165] R. D. Meade, K. D. Brommer, A. M. Rappe, *et al*., "Existence of a photonic band gap in two dimensions," *Applied Physics Letters*, vol. 61, no. 4, pp. 495–497, 1992.

[166] M. Tokushima, H. Kosaka, A. Tomita, *et al*., "Lightwave propagation through a 120 sharply bent single-line-defect photonic crystal waveguide," *Applied Physics Letters*, vol. 76, no. 8, pp. 952–954, 2000.

[167] Y. Akahane, T. Asano, B. S. Song, *et al*., "High-q photonic nanocavity in a two-dimensional photonic crystal," *Nature*, vol. 425, no. 6961, pp. 944–947, 2003.

[168] K. Sakoda, *Optical Properties of Photonic Crystals*. Springer, Berlin, Germany, 2005.

[169] A. B. Khanikaev, S. H. Mousavi, W. K. Tse, *et al*., "Photonic topological insulators," *Nature Materials*, vol. 12, no. 3, pp. 233–239, 2013.

[170] L. Lu, J. D. Joannopoulos, and M. Soljačić, "Topological photonics," *Nature Photonics*, vol. 8, no. 11, pp. 821–829, 2014.

[171] Y. H. Yang, Y. Yamagami, X. B. Yu, *et al*., "Terahertz topological photonics for on-chip communication," *Nature Photonics*, vol. 14, no. 7, pp. 446–451, 2020.

[172] D. Sievenpiper, L. J. Zhang, R. F. J. Broas, *et al*., "High-impedance electromagnetic surfaces with a forbidden frequency band," *IEEE Transactions on Microwave Theory and Techniques*, vol. 47, no. 11, pp. 2059–2074, 1999.

[173] F. R. Yang, K. P. Ma, Y. X. Qian, *et al*., "A uniplanar compact photonic-bandgap (UC-PBG) structure and its applications for microwave circuit," *IEEE Transactions on Microwave Theory and Techniques*, vol. 47, no. 8, pp. 1509–1514, 1999.

[174] F. Yang and Y. Rahmat-Samii, "Microstrip antennas integrated with electromagnetic band-gap (EBG) structures: A low mutual coupling design for array applications," *IEEE Transactions on Antennas and Propagation*, vol. 51, no. 10, pp. 2936–2946, 2003.

[175] F. Yang and Y. Rahmat-Samii, *Electromagnetic Band Gap Structures in Antenna Engineering*. Cambridge University Press, Cam-

bridge, UK, 2010.

[176] S. L. Sun, Q. He, S. Y. Xiao, *et al*., "Gradient-index meta-surfaces as a bridge linking propagating waves and surface waves," *Nature Materials*, vol. 11, no. 5, pp. 426–431, 2012.

[177] B. H. Fong, J. S. Colburn, J. J. Ottusch, *et al*., "Scalar and tensor holographic artificial impedance surfaces," *IEEE Transactions on Antennas and Propagation*, vol. 58, no. 10, pp. 3212–3221, 2010.

[178] D. F. Sievenpiper, J. H. Schaffner, H. J. Song, *et al*., "Two-dimensional beam steering using an electrically tunable impedance surface," *IEEE Transactions on Antennas and Propagation*, vol. 51, no. 10, pp. 2713–2722, 2003.

[179] J. W. You, Q. Ma, Z. H. Lan, *et al*., "Reprogrammable plasmonic topological insulators with ultrafast control," *Nature Communications*, vol. 12, no. 1, article no. 5468, 2021.

[180] Z. B. Popovic, R. M. Weikle, M. Kim, *et al*., "A 100-MESFET planar grid oscillator," *IEEE Transactions on Microwave Theory and Techniques*, vol. 39, no. 2, pp. 193–200, 1991.

[181] R. W. Weikle, M. Kim, J. B. Hacker, *et al*., "Planar MESFET grid oscillators using gate feedback," *IEEE Transactions on Microwave Theory and Techniques*, vol. 40, no. 11, pp. 1997–2003, 1992.

[182] C. F. Jou, W. W. Lam, H. Z. Chen, *et al*., "Millimeter-wave diode-grid frequency doubler," *IEEE Transactions on Microwave Theory and Techniques*, vol. 36, no. 11, pp. 1507–1514, 1988.

[183] J. B. Hacker, R. M. Weikle, M. Kim, *et al*., "A 100-element planar schottky diode grid mixer," *IEEE Transactions on Microwave Theory and Techniques*, vol. 40, no. 3, pp. 557–562, 1992.

[184] J. Lee, M. Tymchenko, C. Argyropoulos, *et al*., "Giant nonlinear response from plasmonic metasurfaces coupled to intersubband transitions," *Nature*, vol. 511, no. 7507, pp. 65–69, 2014.

[185] G. X. Li, S. M. Chen, N. Pholchai, *et al*., "Continuous control of the nonlinearity phase for harmonic generations," *Nature Materials*, vol. 14, no. 6, pp. 607–612, 2015.

[186] W. M. Ye, F. Zeuner, X. Li, *et al*., "Spin and wavelength multiplexed nonlinear metasurface holography," *Nature Communications*, vol. 7, no. 1, article no. 11930, 2016.

[187] E. Almeida, O. Bitton, and Y. Prior, "Nonlinear metamaterials for holography," *Nature Communications*, vol. 7, no. 1, article no. 12533, 2016.

[188] Z. Y. Wang, Z. Wang, J. Y. Wang, *et al*., "Gyrotropic response in the absence of a bias field," *Proceedings of the National Academy of Sciences of the United States of America*, vol. 109, no. 33, pp. 13194–13197, 2012.

[189] S. Taravati, B. A. Khan, S. Gupta, *et al*., "Nonreciprocal nongyrotropic magnetless metasurface," *IEEE Transactions on Antennas and Propagation*, vol. 65, no. 7, pp. 3589–3597, 2017.

[190] A. E. Cardin, S. R. Silva, S. R. Vardeny, *et al*., "Surface-wave-assisted nonreciprocity in spatio-temporally modulated metasurfaces," *Nature Communications*, vol. 11, no. 1, article no. 1469, 2020.

[191] X. C. Wang, A. Díaz-Rubio, H. N. Li, *et al*., "Theory and design of multifunctional space-time metasurfaces," *Physical Review Applied*, vol. 13, no. 4, article no. 044040, 2020.

[192] S. Taravati and G. V. Eleftheriades, "Full-duplex nonreciprocal beam steering by time-modulated phase-gradient metasurfaces," *Physical Review Applied*, vol. 14, no. 1, article no. 014027, 2020.

[193] R. E. Meymand, A. Soleymani, and N. Granpayeh, "All-optical AND, OR, and XOR logic gates based on coherent perfect absorption in graphene-based metasurface at terahertz region," *Optics Communications*, vol. 458, article no. 124772, 2020.

[194] N. Hu, Y. T. Zhao, J. H. Zhang, *et al*., "High-performance energy selective surface based on equivalent circuit design approach," *IEEE Transactions on Antennas and Propagation*, vol. 70, no. 6, pp. 4526–4538, 2022.

[195] H. Wakatsuchi, S. Kim, J. J. Rushton, *et al*., "Waveform-dependent absorbing metasurfaces," *Physical Review Letters*, vol. 111,

no. 24, article no. 245501, 2013.

[196] L. L. Dai, B. C. Wang, M. Wang, *et al*., "Reconfigurable intelligent surface-based wireless communications: Antenna design, prototyping, and experimental results," *IEEE Access*, vol. 8, pp. 45913–45923, 2020.

[197] M. Di Renzo, A. Zappone, M. Debbah, *et al*., "Smart radio environments empowered by reconfigurable intelligent surfaces: How it works, state of research, and the road ahead," *IEEE Journal on Selected Areas in Communications*, vol. 38, no. 11, pp. 2450–2525, 2020.

[198] Q. Cheng, L. Zhang, J. Y. Dai, *et al*., "Reconfigurable intelligent surfaces: Simplified-architecture transmitters—from theory to implementations," *Proceedings of the IEEE*, vol. 110, no. 9, pp. 1266–1289, 2022.

[199] J. W. Tang, M. Y. Cui, S. H. Xu, *et al*., "Transmissive RIS for 6g communications: Design, prototyping, and experimental demonstrations," *arXiv preprint*, arXiv: 2206.15133, 2022.

[200] C. Liu, Q. Ma, Z. J. Luo, *et al*., "A programmable diffractive deep neural network based on a digital-coding metasurface array," *Nature Electronics*, vol. 5, no. 2, pp. 113–122, 2022.

Changhao Liu received the B.S. degree in electronic engineering from Tsinghua University, Beijing, China, in 2021, where he is currently pursuing the Ph.D. degree in electronic engineering. From 2019 to 2021, he was a Research Assistant at the Microwave and Antenna Institute, Department of Electronic Engineering, Tsinghua University. His current research interests include reconfigurable metasurfaces, surface electromagnetics, reflectarray antennas, transmitarray antennas, and terahertz metasurfaces. (Email: liu-ch21@mails.tsinghua.edu.cn)

Fan Yang received the B.S. and M.S. degrees from Tsinghua University, Beijing, China, in 1997 and 1999, respectively, and the Ph.D. degree from the University of California at Los Angeles (UCLA), Los Angeles, CA, USA, in 2002.

From 1994 to 1999, he was a Research Assistant at the State Key Laboratory of Microwave and Digital Communications, Tsinghua University. From 1999 to 2002, he was a Graduate Student Researcher at the Antenna Laboratory, UCLA. From 2002 to 2004, he was a Post-Doctoral Research Engineer and an Instructor at the Department of Electrical Engineering, UCLA. In 2004, he joined the Department of Electrical Engineering, The University of Mississippi, Oxford, MS, USA, as an Assistant Professor, where he was promoted to an Associate Professor in 2009. In 2011, he joined the Department of Electronic Engineering, Tsinghua University, as a Professor, where he has been the Director of the Microwave and Antenna Institute since 2011. He has published over 300 journal articles and conference papers, 6 book chapters, and 5 books entitled *Reflectarray Antennas: Theory, Designs, and Applications* (IEEE-Wiley, 2018), *Analysis and Design of Transmitarray Antennas* (Morgan & Claypool, 2017), *Scattering Analysis of Periodic Structures Using Finite-Difference Time-Domain Method* (Morgan & Claypool, 2012), *Electromagnetic Band Gap Structures in Antenna Engineering* (Cambridge University Press, 2009), and *Electromagnetics and Antenna Optimization Using Taguchi's Method* (Morgan & Claypool, 2007). His research interests include antennas, surface electromagnetics, computational electromagnetics, and applied electromagnetic systems.

Dr. Yang is a Fellow of the Applied Computational Electromagnetics Society (ACES). He was a recipient of several prestigious awards and recognitions, including the Young Scientist Award of the 2005 URSI General Assembly and the 2007 International Symposium on

Electromagnetic Theory, the 2008 Junior Faculty Research Award of the University of Mississippi, the 2009 inaugural IEEE Donald G. Dudley Jr. Undergraduate Teaching Award, and the 2011 recipient of Global Experts Program of China. He was the Technical Program Committee (TPC) Chair of the 2014 IEEE International Symposium on Antennas and Propagation and the USNC-URSI Radio Science Meeting. He served as an Associate Editor for the *IEEE Transactions on Antennas and Propagation* from 2010 to 2013 and the Associate Editor-in-Chief for *Applied Computational Electromagnetics Society (ACES) Journal* from 2008 to 2014. He is a Distinguished Lecturer of IEEE Antennas and Propagation Society (APS), since 2018.
(Email: fan_yang@tsinghua.edu.cn)

Shenheng Xu received the B.S. and M.S. degrees from the Southeast University, Nanjing, China, in 2001 and 2004, respectively, and the Ph.D. degree in electrical engineering from the University of California at Los Angeles (UCLA), Los Angeles, CA, USA, in 2009.

From 2000 to 2004, he was a Research Assistant with the State Key Laboratory of Millimeter Waves, Southeast University. From 2004 to 2011, he was a Graduate Student Researcher and later a Post-Doctoral Researcher with the Antenna Research, Analysis, and Measurement Laboratory, UCLA. In 2012, he joined the Department of Electronic Engineering, Tsinghua University, Beijing, China, as an Associate Professor. His research interests include novel designs of high-gain antennas for advanced applications, artificial electromagnetic structures, and electromagnetic and antenna theories.
(Email: shxu@tsinghua.edu.cn)

Maokun Li received the B.S. degree in electronic engineering from Tsinghua University, Beijing, China, in 2002, and the M.S. and Ph.D. degrees in electrical engineering from the University of Illinois at Urbana–Champaign, Champaign, IL, USA, in 2004 and 2007, respectively. After graduation, he worked as a Senior Research Scientist with Schlumberger-Doll Research, Cambridge, MA, USA. Since 2014, he has been with the Department of Electronic Engineering, Tsinghua University. He has authored or coauthored one book chapter, 50 journal articles, and 120 conference proceedings. He holds three patent applications. His research interests include fast algorithms in computational electromagnetics and their applications in antenna modeling, electromagnetic compatibility analysis, inverse problems, and so on.

Dr. Li was a recipient of the China National 1000 Plan in 2014 and the 2017 IEEE Ulrich L. Rohde Innovative Conference Paper Award. He serves as an Associate Editor for the *IEEE Journal on Multiscale and Multiphysics Computational Techniques* and *Applied Computational Electromagnetic Society Journal* and a Guest Editor for the Special Issue on Electromagnetic Inverse Problems for Sensing and Imaging of the *IEEE Antennas and Propagation Magazine.*
(Email: maokunli@tsinghua.edu.cn)